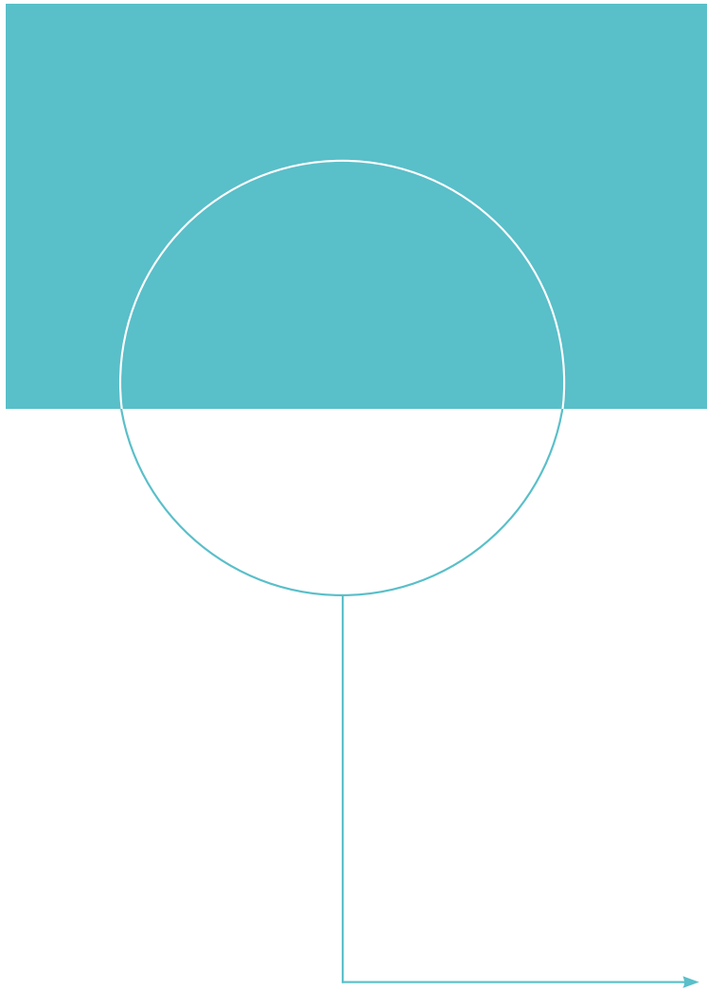

Master's thesis

2020

Marianna Kalogeropoulou

NTNU
Norwegian University of
Science and Technology
Faculty of Engineering
Department of Civil and Environmental Engineering

Marianna Kalogeropoulou

Back calculation of the Sørkjosen's landslide

USING PLAXIS

June 2020

NTNU
Norwegian University of
Science and Technology

NTNU
Norwegian University of
Science and Technology

NTNU

Norwegian University of
Science and Technology

Back calculation of the Sørkjosen's landslide

USING PLAXIS

Marianna Kalogeropoulou

Geotechnics and Geohazards
Submission date: June 2020
Supervisor: Steinar Nordal

Norwegian University of Science and Technology
Department of Civil and Environmental Engineering

ABSTRACT

Norway is exposed to frequent landslide activity. A large number of landslides occur each year, causing damage to infrastructure, or even loss of lives. Due to the changing climate and the extreme weather patterns, the landslide activity in Norway is expected to increase.

A shoreline landslide with a volume up to 1,4 million m3 took place at Sørkjosen, a village in Troms and Finnmark county, at the night from the 9th to the 10th of May 2015. The shoreline slid into the sea over more than 1 km and parts of the local harbor were destroyed. No persons were killed but after the landslide the traffic had to take a 700km detour through Finland to pass the site. The slide occurred in a fjord with steep slopes and a large river delta. Also, there were ongoing road construction prior to the event, including rock blasting.

Some of the destabilizing factors are presented below:

- Filling and roadworks
- Low tide
- Precipitation (24,9 mm)
- Excess pore pressure (10kpa)

The main objective of this report is to gain a greater understanding for this event. Undrained analysis is carried out in the finite element method program 'Plaxis 2D'. In the investigation that took place in 2016 (Nordal.S, L'Heureux.J, Skotheim. A, 2016) NGI-ADP material model was used for the stability calculations. In this report the Mohr- Coulomb material model has been used for various simulations with constant and varying undrained shear strength of the clay layer.

The simulations must be regarded as containing significant simplifications on the real slide event, as they do not account for three- dimensional effects.

PREFACE

The following master thesis marks my final work of the study program MSc. Geotechnics and Geohazards. The work has been conducted for the Department of Civil and Environmental Engineering at NTNU. The study was carried out during the spring semester of 2020.

A literature review concerning landslides and simulations for the back-calculation of the landslide are included in the present Master Thesis.

The overall theme of the thesis are submarine landslides along the shoreline, with special focus on the landslide that took place in Sørkjosen on May 10th, 2015.

ACKNOLEDGMENTS

Firstly, I would like to thank my supervisor, Professor Steinar Nordal, for his guidance both throughout the master's degree and during our cooperation at the present master thesis. The understanding that he showed and the multifaceted assistance, when I needed, was significant.

My sincere thanks go to many friends and colleagues, not only for scientific discussion but also for the great and challenging times we shared during our studies. I only name a few of them with whom I spent a considerable amount of time working on projects and studying for exams. These are Mushfiq Hassan and Bea Almarza.

I must gratefully acknowledge other personal friends, like Konstantina Sidiropoulou, Dimitra Visvikou, Lia Voutsina and many more for the great times and memorable moments we had. I believe my joyful free time during university was a necessity to stay focused and fully energized while studying and researching.

Finally, the biggest thank you goes to my parents and siblings, Katerina and Panagiotis for their mental and psychological support.

Table of contents

List of figures

List of tables

1. Introduction

The term ‘landslide’ refers to natural downwards movements which can contain a wide range of soil material. Rockfalls, rock slides, snow avalanches, debris flows and quick clay slides are some of the types or movements that the term ‘landslide’ can refer to. Landslides can be destructive for the urban infrastructures or/and for human losses.

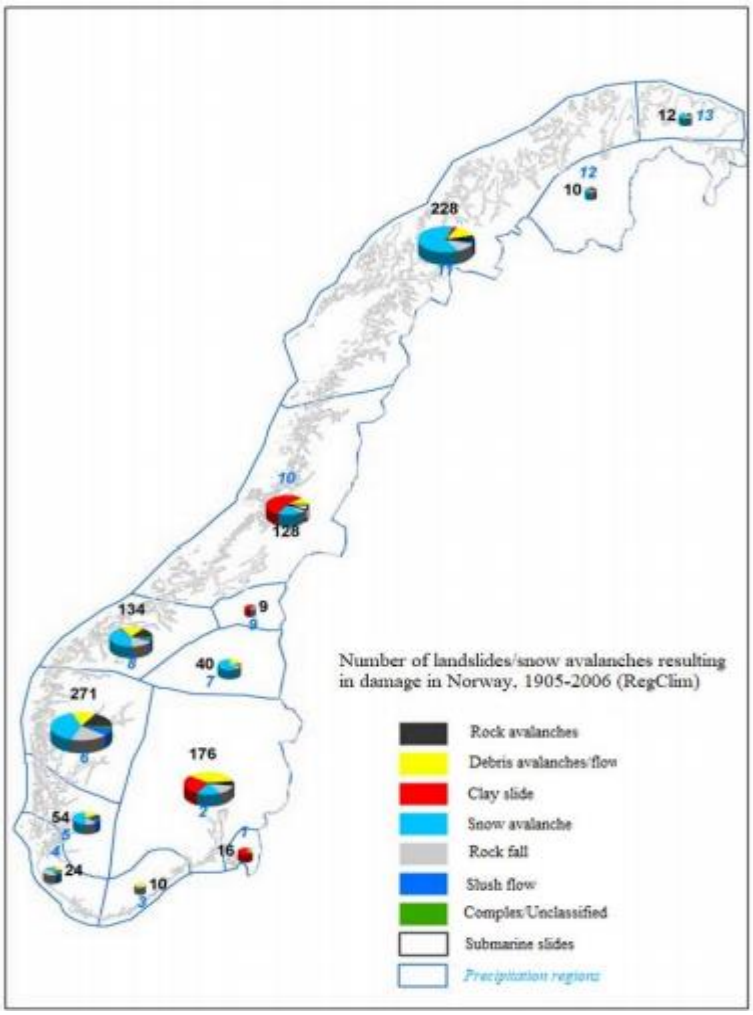

There are many reasons which can be responsible for a landslide event. Geological formations and human intervention are the major causes of a landslide. The most common types of landslides in Norway are quick clay flows, rock falls and snow avalanches (Thakur, V. Yifru.A,2014). Along the Norwegian road network, 1 500 – 2 000 incidents of sliding activity were recorded per year in the period between 2000 and 2009 (Bjordal et.al.,2011). Between 2004 - 2016, there have been five fatalities due to landslides in soils, and it is estimated that about 125 fatalities have occurred over the past 150 years (Colleuille et al., 2017).

Recently, a very important type of landslide is studied. Submarine landslides can be proved as disastrous as the other types mentioned above.

Figure 1: Damage statistics in Norway. Modified from (Hovelsrud et al., 2007).

1.1 Background

Landslides that occur on the seabed have been a field of interest in Norway for a long time because many people are living along the coast but also because of the investigation of oilfields on seabed. The depositional history of Norway, with large quantities of quaternary geological materials combined with the steep topography make the country prone to significant landslides. This also applies on the sea floor. The submarine landslides have inflicted many coastal environments and have caused enormous damage both in the form of material destruction and loss of human life. In the presence of quick clay, these landslides have proven to be further dramatic.

A characteristic of submarine landslides is that they often remain extensive, both in length along the shoreline and in volume of mobilized masses.

This master thesis deals with an underwater landslide that took place in 2015. The landslide occurred at Sørkjosen, a village in Troms and Finnmark county. The slide carried along parts of the shoreline along the E6 from the pier to Jubelen (figure 2).

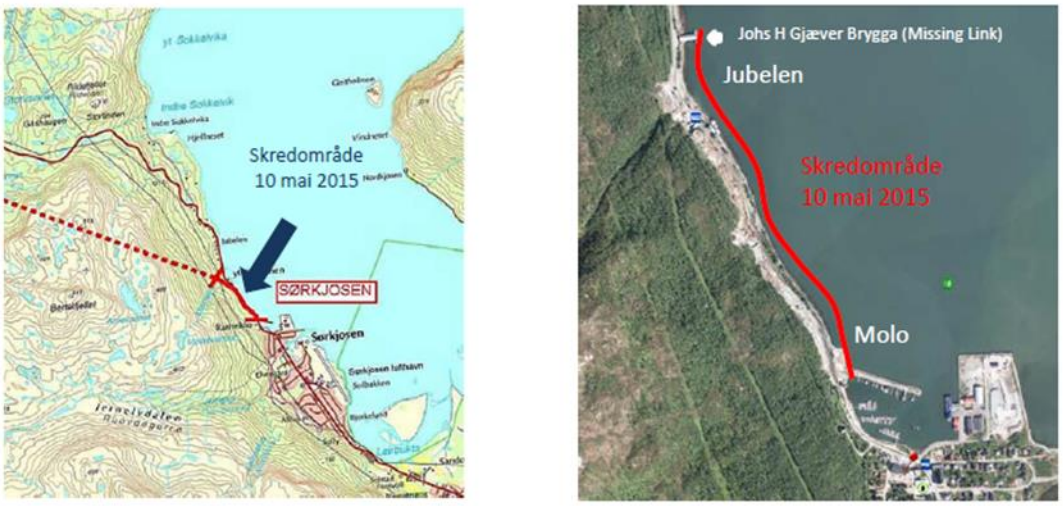

Figure 2 : The landslide area is between the tunnel at Jubelen and a pier north of the center of Sørkjosen. The shoreline along the E6 is affected for a length of approx. 1000 meters. (Map is taken from the 2012 zoning plan for E6 Sørkjosenfjellet and from finn.no/kart).

1.2 Problem Description

The main goal of this report is to gain a greater understanding of the landslide event in Sørkjosen. It is necessary to map what kind of basic conditions were present and enabled the landslide development along the shoreline.

The scope of work for the investigation includes the following work items:

- Review Available Information: Reports, maps, and construction records were reviewed for information pertaining to local and regional geology, slope stability, and bathymetry.
- Plaxis 2D simulations to further understand the landslide event.

The questions that have been posed in this thesis are:

- Back calculations for slope stability with the Plaxis software (Mohr Coulomb criterion used as material model).
- How the shear strength anisotropy influences the slope stability calculations.

1.3 Limitations

Result analysis may be limited by insufficient statistical and mathematical knowledge. Furthermore, another limitation of the thesis is that it focuses strongly on the obtained field data. Also, the analysis chapter places great emphasis on analyzes in the Plaxis 2D program and to a certain degree, the report is not too critical to the calculation results. Finally, only one soil profile is modelled (profile 31 in appendix 1), and other areas affected by the landslide are not taken into consideration in the simulations. The model created in Plaxis is a simplified version of profile 31.

1.4 Report composition

Overview of the structure of the report:

- Abstract
- Preface
- Acknowledgments
- Chapter 1: Introduction

- Chapter 2: Literature review – the purpose of this part is to present a relevant theoretical basis of the mechanism and principles governing landslide processes, especially submarine ones.
- Chapter 3: Theory. This chapter deals with shear strength anisotropy and a theoretical background of the software, Plaxis, which is used in this thesis.
- Chapter 4: Case study. Available information regarding the landslide event in Sørkjosen.
- Chapter 5: Calculations with Plaxis software.
- Chapter 6: Discussions, Conclusions and Recommendations for further work.
- Bibliography
- Appendix

2. Literature review

Chapter 2 is a literature study of landslides with specific focus in submarine ones. Chapter 2.1 presents landslide characteristics, including classification and morphology. Chapter 2.2 analyses submarine landslides, Chapter 2.3 deals with triggering mechanisms and chapter 2.4 refers to Fjord- delta geomorphology.

2.1 Landslide classification

Landslide is a broad term which describes a variety of processes. A common definition is *'the failure and movement of a mass of rock, soil, or artificial fill under the influence of gravity'* (Clague, 2013). More specific definitions may be used to communicate the characteristics of different types of landslides. These definitions and classifications are mainly based on how the displaced mass is moving and/or what type of material the displaced mass consists of. A widely used classification system is the one proposed by (Varnes, 1978), which divides the types of mass movements into five classes and the type of mass into three materials: rock,

debris, and earth. Debris is defined as a material in which 20-80 % of the grains are larger than 2mm, with the remainder of the fragments less than 2mm in size (Shroder, 1971). Earth is defined as a material in which at least 80% of fragments re smaller than 2mm.

The categories based on the type of mass movement are presented below.

Fall

The detachment of a mass of soil or rock from a steep slope is considered a fall. There is little or no shear displacement along the failure surface before the detachment. The material will mainly descend by falling, bouncing, or rolling (Highland and Bobrowsky, 2008). The main causes are gravitational forced, differential erosion or excavation works.

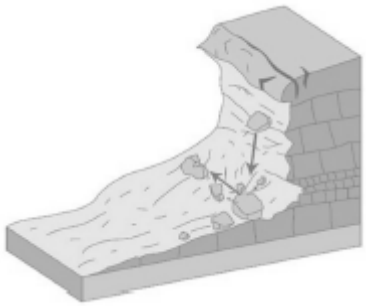

Figure 3: Fall

Topple

A mass of soil or rock, forward rotating around a point or axis below its center of gravity describes a topple-like movement type (Highland and Bobrowsky, 2008). The speed of topple motion can vary from slow to extremely fast and it is mainly met in rock slopes. On the contrary, debris and earth topples are rare events and the occurrence of these is due to either natural processes or human interventions.

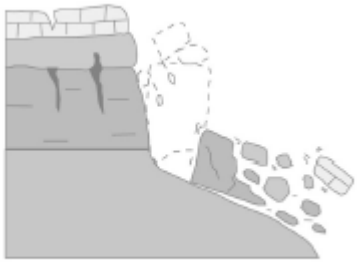

Figure 4: Topple

Slide

A mass of soil or rock moving downslope on surfaces of rupture, or thin regions of intense shear displacement represents a slide like event. The movement of the entire mass does not occur simultaneously, but grows from its local point of origin, mobilizing a larger volume along its path (Highland and Bobrowsky, 2008). The slide is rotational if it has a curved surface of ruptured, where the displaced mass has rotated about an axis at a right angle to its vertical cross-section. If the displaced mass follows a planar surface, with little rotational movement it is called a translational slide (Highland and Bobrowsky 2008) or planar slide (Hungr et. Al. 2014).

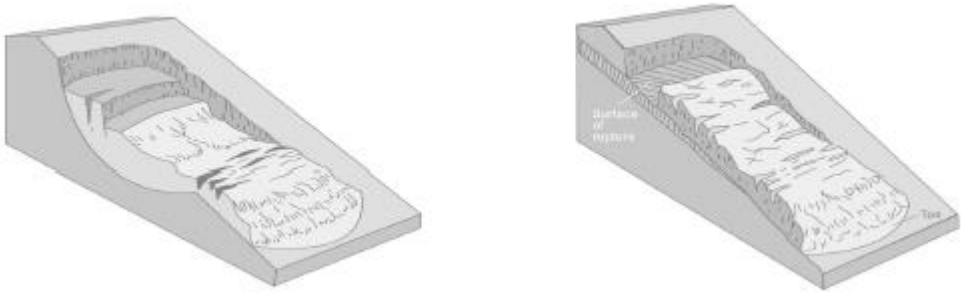

Figure 5: Left side- rotational slide, Right side – Planar slide.

Flow

A continuously moving mass, behaving like a viscous liquid characterizes the flow like movement types. The shear surfaces are closely spaced, short lived and usually not preserved (Highland and Bobrowsky, 2008). Rock, debris, and earth flows are possible to occur. In rock flows, small deformations are observed that are distributed in either small or bigger cracks but without any sign of displacement along a surface. They usually spread in small distances.

On the other side, debris and earth flows are easily recognized as they run in bigger distances and they are intense due to high cohesive material content. They are a fast mass movement in which a combination of uncompacted soil, rock, organic elements, air, and water is flowing in a downwards surface. Debris flow are mainly caused by the high water flows due to extreme precipitation on the rapid snow melting which erodes and mobilize the loose material or the rock in steep slopes.

Finally, if flows have extremely slow velocities they are classified as creep. Creep is indiscernible rather than stable and downwards mass movement.

rather than stable and downwards mass movement. There are three categories of creep, seasonal,

Figure 6: Debris flow

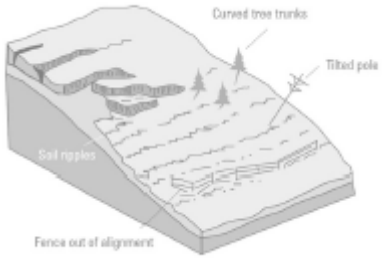

Figure 7: Creep

2.2 Submarine landslides

Submarine landslide is a mechanism where sediments collapse and settle in deeper sea level. The length of this landslides can reach up to several hundred kilometers. The volume of an average subsea landslide also tends to be larger than the average landslide (Elverhøi et al.2002). The largest known submarine landslide is Storegga. The slide occurred on the Norwegian continental shelf with slope angle below 1°. Landslide masses are estimated to be 6.000km^3 m^3 (Kvalstad et al, 2005).

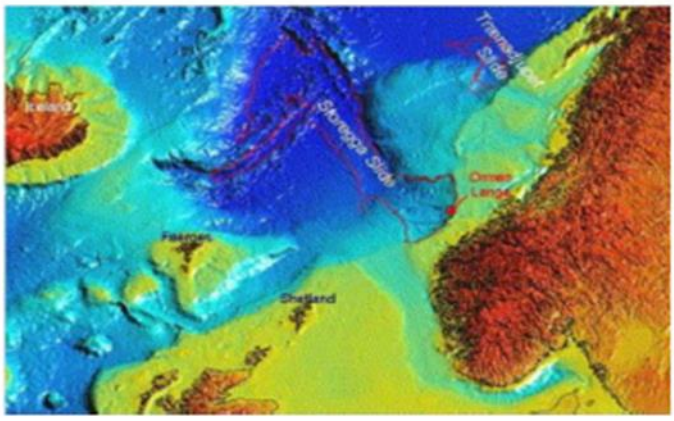

Figure 8: Storegga landslide (Kvalstad et al. 2005).

During the years, many researchers pointed different causes of a submarine landslide. According to Locat and Lee (2000) some of them can be:

- Over – Steepening
- Seismic loading
- Storm – Wave Loading
- Rapid accumulation and Under Consolidation
- Low tides
- Seepage
- Gas charging
- Gas Hydrate Disassociation
- Glacial Loading
- Volcanic island processes

Submarine landslides can be studied from a geotechnical scope (Lerouil, Locat et al. 1996). However due to their complexity and their multilevel phases different principles are applied. Soil and rock mechanics, torrential hydraulics or fluid mechanics principles can have an application on the study of a submarine landslide (Locat and Lee 2000).

Globally, earthquakes are one of the most common causes of subsea landslides. This trigger is not focused on this task, since Norway has generally a very small number of earthquakes (Elverhoi et al, 2002).

Underwater landslides often occur at low tide. This is because at that time the back pressure from the water on the slope is lower and the flow pressure in the masses increases (Andresen and Bjerrum, 1967). The driving forces in the slope's soil are maximal. At low tide, gas in sediments can be included. Organic material expands and lead to rupture (Talling et. Al, 2014).

2.3 Triggering Mechanisms

The cause of a landslide is a result of complex processes. Natural and human activities can both trigger a landslide event. Generalized processes, that can case a landslide have been classified and presented below (Brunsden et. Al 1993).

External process	Causal process	Description
Weathering *(Physical, chemical and biological)*	Physical properties	Changes in particle size
	Chemical properties	Cation exchange, cementation
	Horizonation	Internal layers, ripening, weaker discontinuities
	Regolith thickness	Often determined by slope shape
Erosion *(Fluvial, glacial, coastal etc.) Material removal from face or base of slope.*	Geometrical change	Relief, height, length, angle, aspect
	Unloading	Removal of lateral support, expansion, swelling, fissuring, strain softening, stress concentration
Ground subsidence	Undermining	Mechanical eluviation of fines, leaching, removal of cement, seepage erosion
Deposition *(Fluvial, glacial, mass movement etc.) New material added to face or top of the slope.*	(Undrained) Loading	Landslide activity, deltaic addition, talus accumulation
Shocks and vibration	Vertical and horizontal movement	Varying frequency, magnitude, intensity, duration, disturbance to intergranular bonds and cement, water table change
Air fall *Wind-blown sediments, loess Volcanic sediments, tephra*	Addition of fine components to the soil. Mantling with fine regolith.	Producing a new slope with the old surface as possible shear zone
Water regime change *(Geomorphological or meteorological)*	Surface saturation.	Flooding, lake bursts, etc.
	Water-table, and pressure change.	"Wet" rainfall years, intense precipitation, snow and ice melt, drawdown
Compound *Possible "follow-on" or run out processes after initial failure, e.g. after bank collapse, etc.*	Liquefaction, remolding, cohesionless grain flow, heat generation, rate effects, chemical effects.	

Table 1 : Classification of contributed processes to the triggering of a landslide (Brunsden 1993)

In Norway, some of the main causes for landslide events are weak zones, clay layers, sand and gravel layers and pore pressure. In the next chapters this causes will be analyzed.

2.3.1Weak zones

A definition of a weak layer is proposed here using a geotechnical perspective: a layer (or band) consisting of sediment or rock that has strength potentially or actually sufficiently lower than that of adjacent units (strength contrast) to provide a potential focus for the development of a surface of rupture. Such a layer or a band can follow stratigraphic horizons, but this is not a requirement. From this it is proposed to define two types: inherited and induced weak layers. Also, silt can liquify, when disturbed and represent a weak zone, in particular if capped by an almost impervious clay layer. In addition, weak layers can develop in strain softening sediments where progressive failure can generate a surface of rupture without the need to invoke the role of excess pore pressures. Under critical circumstances, the sliding surface of a rupture may occur here (Locat et al, 2014). Weak layers can be formed by sedimentation, geotechnical and geochemical processes (L'Heureux and NTNU, 2009).

Geotechnical surveys combined with high resolution bathymetry and date from seismic reflections are the best methods for identifying week zones.

2.3.2Clay layers

Studies have shown that some large submarine landslides in fjord environments have occurred nearby of or along weak clay layers. These layers have usually been formed by rapid changes in the environment. Whether for a short period of abnormally rapid sedimentation, (Locat et al., 2014) or they may have occurred following an event that led to rapid deposition of masses; previous landslides, earthquakes, floods, or storms. (Hansen et al., 2011)

In thick deposits of clay can be found layers of quick clay, and if the failure occur there the slide will move fast. Layers of quick clay can be found in sidewalls along the fjord and by the slope of a delta. (Locat et al., 2014) These layers can be very difficult to detect since they can be thin. The layers can be detected on seismic reflection and on the CPTU.

2.3.3Sand- gravel layers

Layers that have low or no cohesion can also develop sliding planes. Friction soils have often a more open structure than cohesive ones. This allows gas hydrates to accumulate in the open structure. If the pore pressure increases, the gas contained in these layers can flow out and the layer can collapse. Increased pore pressure in such layers will also cause the effective stress to decrease and the strength of the slope decreases. A layer of gravel and sand can also form a flow channel if nearby soils are less permeable. The water flow will decrease the effective stresses, and in the worst case can cause the grain contact to disappear and to completely lose all its shear strength. (Locat et al., 2014) Shaking or vibration in loosely stored sand and gravel can also potentially result in the shear strength disappearing. (Andresen and Bjerrum,1967).

Landslides that have occurred into friction earth soils can be difficult to make good stability calculations on as the calculations can give an unrealistically high material factor. (Andresen and Bjerrum, 1967) Knowledge of pore overpressure in such soils is therefore necessary.

2.3.4Pore Pressure

A decisive factor for stability is the pore pressure distribution on the slope. Increase in pore pressure leads to reduced effective stresses, see Figure 9. When the pore pressure becomes so large that it carries all the overlying weight, then a failure will occur.

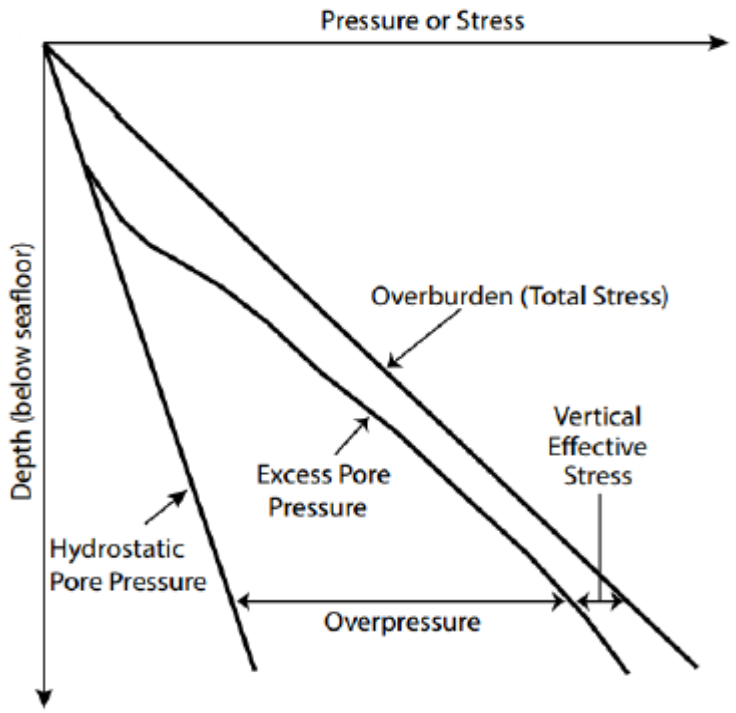

Figure 9: Example of how the pore pressure can increase with depth and reduce the effective stresses (Talling et.al,2014).

Pore overpressure occurs when the liquid in one layer or area cannot flow to another area with lower potential. Low permeability layers prevent this flow. Increased pore pressure can be due to rapid sedimentation or flow in loose layers below dense / impermeable layers. (Talling et al., 2014) Increased pore pressure can initiate retrogressive and progressive landslides, see Figure 10.

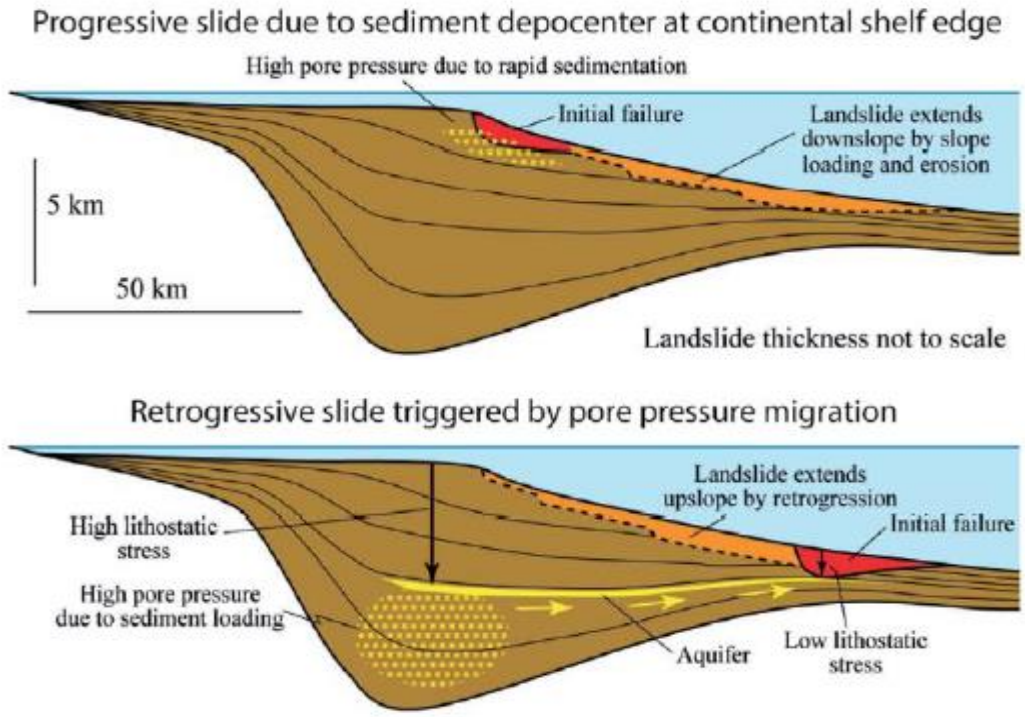

Figure 10: Pore overpressure in the beach zone (Masson et, al, 2010).

If you have no data from pore pressure measurements, the pore pressure situation must be estimated based on topography and other knowledge of basic conditions. In areas where one with overpressure in deeper layers, you will occasionally be able to see pockmarks off the shoreline. Pockmarks are formed by short-term outflow of gas or groundwater from deeper layers, they can be seen in bathymetry as circular holes. Pockmarks can be tens of meters in diameter. (L'Heureux et al., 2012b).

Many natural slopes can be close to eruption, especially if a stream or waves dig in the slope. Critical condition can then occur at high pore pressure in the soil, for example, during heavy rain or snow melt. (Emdal et al., 2015)

Studies from 2003 describe that the landslide in Finneidfjord have been triggered when an initial slide went into a weak layer with high pore pressure. The layer was continuous and was between 1-9 meters under the seabed. The initial slide has affected the quick clay in the beach zone, by relief, given one adverse slope angle and / or eroded the quick clay. Initial slide triggered a retrogressive landslide development in Finneidfjord. (Longva et al., 2003).

Recent research has shown that the weak layer of landslide that have occurred along, is a layer of sensitive clay (L'Heureux et al., 2012b). In Finneidfjord, also, artesian pore pressure has been

occurred in the soil. This pore pressure has among other things, gathered under the impermeable clay layers, and led to a reduction in effective stresses. An overpressure of 8kPa is found 3 meters below sea level in Finneidfjord. (L'Heureux et al., 2012b) The reason for the landslide in Finneidfjord has been found to be a combination of high pore pressure in the soil and human activity in the beach zone, filling.

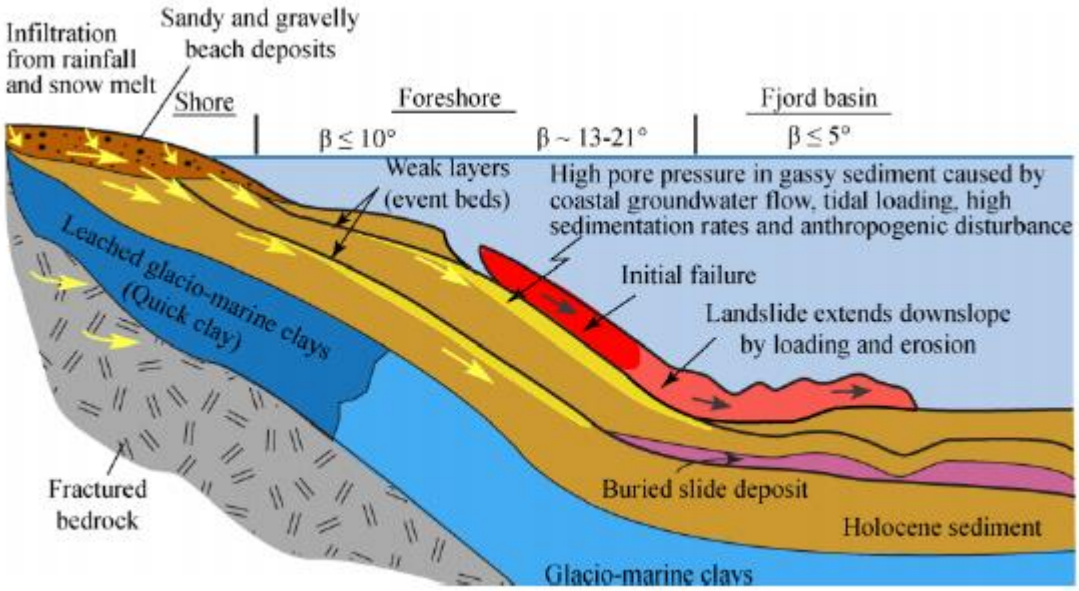

Figure 11: Schematic illustration of the various factors that can affect slope stability. (L'Heureux et al., 2012b)

2.4 Fjord- Delta geomorphology

Fjords in Norway are mainly formed during and after the last ice age, when the sea "invade" the valley causing the erosion of the valley's floor (Nesje, 1994). Figure 12 presents an example of a fjord formation with phases. In some cases, a fjord can 'meet' with a delta (Hampton et.al 1996). Deltas are distinctive geological formations shaped at the mouths of large rivers, when sediments accumulate rather than being washed away by currents or ocean waves. Over time a complex set of channels, sand barriers and marshes format the mouth of the river. In Norway, the deltas grow faster in the spring as the water flows in the rivers in greater volume (Eilertsen et al. 2012).

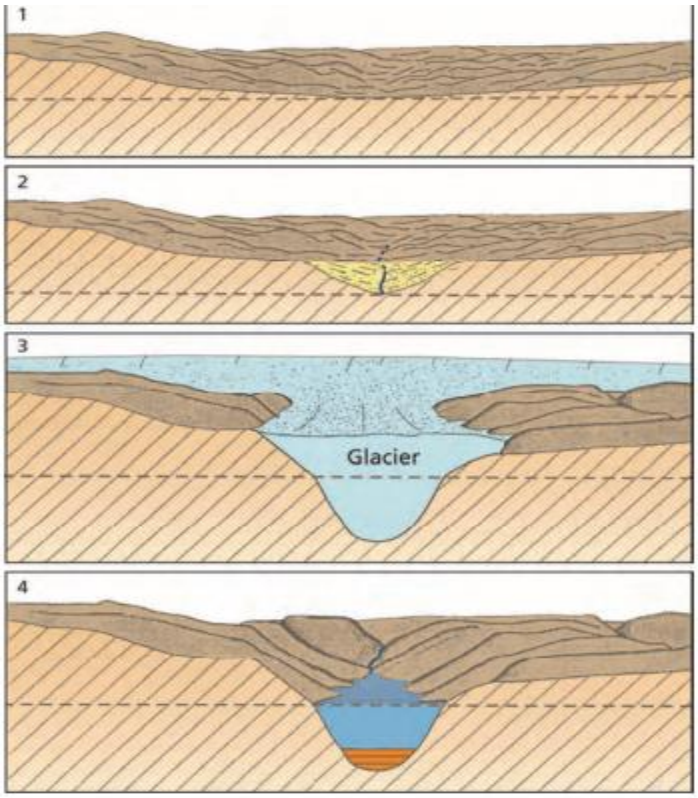

Figure 12: Proposed phases in fjords formation (Nesje & Whillans 1994).

Sea level is represented by the dash line.

The delta plain is crossed by the main channel of the river, which can also branch into narrower channels. In figure the main structure (stratigraphy) of a delta is presented. The timelines illustrate former seabed.

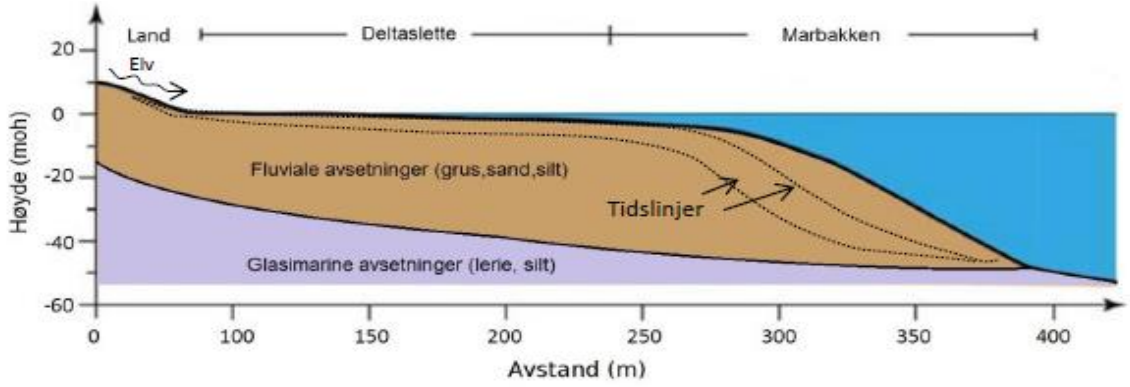

Figure 13: General model of deltas. (L'Heureux et al., 2012a)

2.5 Examples of landslides along the Norwegian fjords

2.5.1Orkdal fjord, Trøndelag

In May 1930, a landslide occurred in the Orkanger beach zone at the Orkdal fjord. The event consisted of several nearby landslides, which were triggered by short time intervals. The total landslide volume was over 18 million m^3. At the port area a 15m high tidal wave was generated. The outcome was very devastating, with major material damage and one death. The causes of the slide were a landfill work combined with natural causes (steep slopes) (L'Heureux et.al, 2014) .

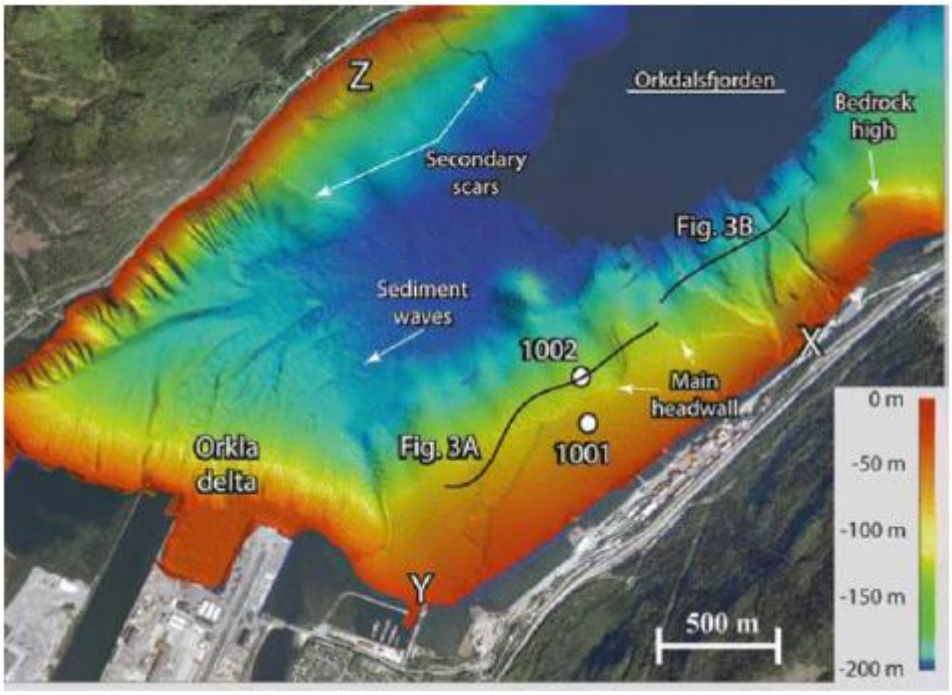

Figure 14: The total landslide area after the incident in the Orkdal fjord (L'Heureux et.al 2014).

2.5.2Finneid fjord, Nordland

In 1996, a landslide occurred in the beach zone in Finneid fjord. It is estimated that 1 million m^3 masses were mobilized and the event ended with 4 fatalities. The slide was initiated on the fjord, in the steepest part of the slope and propagated 150m inland, by backward development (L'Heureux et.al, 2012; Hansen et al,2013).

Preliminary investigations before the landslide recorded soft, sensitive clays with elements of silt, underlying one sand layer with up to 5m thickness. Quick clay was detected also (Longva et.al, 2013). A clay zone collapsed and triggered the initial rupture, which resulted in a rapid clay slide propagating inward. Pore overpressures from heavy rainfall has also been an important cause for the incident, while human activity (filling and blasting on the beach) was also a main cause (Longva et.al, 2013).

This incident is a reminder of how weaker layers in stratigraphy are playing a huge role for beach zone stability (details in chapter 2.3.1). The landslide studied in this paper has a similar stratigraphy with a clay, weak layer, which also played a main role to the slide event.

2.5.3Inner Sokkelvik, Troms

In May 1959, a landslide took place in Sokkelvik, in the beach zone of the Reisa fjord in Troms. Nine people lost their life because of the incident. An important cause was the heavy volume of rainfall and snowmelt the hours before the slide. It is also believed that three local streams have eroded the seabed sufficiently to destabilize the masses to a certain degree. Also, low tide was recorded shortly before the landslide. The main trigger for the landslide, though, was a road construction in the area (7,5 m high filling built six months before the incident),(L'Heureux, Nordal and Austefjord, 2017).

Basic studies from the landslide showed a 3m sand layer over a soft, sensitive clay (L'Heureux, Nordal and Austerfjord, 2017). Bathymetric measurements interpretation from 2006 reveal that the landslide occurred in two stages. Masses have moved south along the coastal zone and spread ashore by retrogression (figure 15).

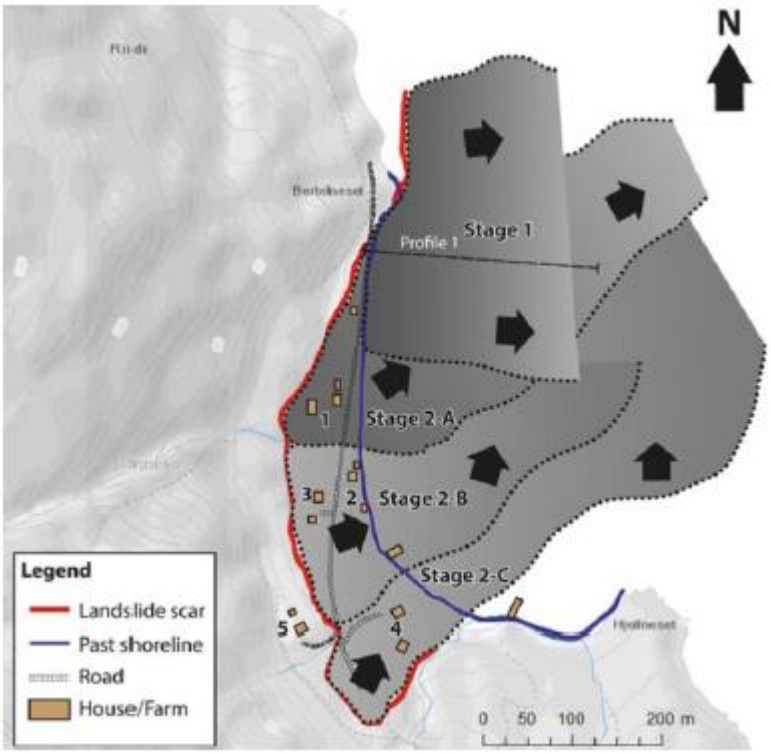

Figure 15: Overview of the landslide in Reisafjord. The arrows illustrate the direction of sliding on the masses (L'Heureux, Nordal and Austefjord, 2017).

The landslide studied in this paper happened only 3 km south in the Reisa fjord. Both landslides occurred under similar conditions. The main cause that triggers both incidents was roadworks (filling work near both areas).

3. Theory

Natural slopes exposed to sufficient destabilizing conditions can lead to failure, which can happen either drained or undrained. These states in geotechnical context describe whether the pore water in a soil element can flow out. For low-permeable soils, pore water is prevented from leaving the material, which provides an undrained state. When such materials experience a rapid load change there is an increase in pore pressure, which leads to pore overpressure. In the other hand, for materials with high permeability, the pore water can infiltrate the soil without obstacles. Slow increase in load of such soils will give full drainage condition. Drained and undrained conditions are two extremes. Real life situations usually will be located somewhere in between, with partially drained conditions (Sandven et.al. 2017).

The landslide in Sørkjosen (Brinkgreve R.B.J., 2010) happened rapidly, which leads to the fact that the pore water in the clay did not allow time to flow out and it failed in an undrained state.

3.1 Drained / Undrained failure

It is important to distinguish between drained and undrained conditions. If the soil pores are saturated with water, failure, depending on the soil pore size, the degree of water saturation and time involved, can take place drained or undrained. The smaller the pores and the faster the loads are applied the more likely that the failure characteristics are undrained.

To explain this in more detail, water, compared to air or unsaturated soil, has a very high bulk modulus. In fact, from a soil engineering point of view, water be incompressible. If the soil pore volume is filled with air, an increase in stress generally results in a compression of air and therefore a total volume change. This is the case for elastic as well as plastic deformation. The volume can either increase or decrease and the this means that the situation is almost drained. On the other hand, if the soil is fully saturated with water and there is not enough time or no possibility for the water to be displaced, the volume stays constant. Only deviatoric volume changes are possible. This means, the soil can purely be deformed but the volume stays constant. For such conditions, the term undrained is used.

To calculate the undrained shear strength for Coulomb's failure criteria and plain strain conditions one can use the following equation:

$$su = c' * \cos(\varphi') + \left(\frac{\sigma 1+\sigma 3}{2}\right) * \sin(\varphi') \qquad (1)$$

One of today' most common failure criteria, that assumes constant shear strength is the Tresca failure criterion (H., 1868). Figure 16 illustrates Tresca criterion in a σ- τ diagram. Additionally, the relationship between su and the drained strength parameters is presented (plane strain). Furthermore, the two stress circles represent am effective and total stress state, respectively.

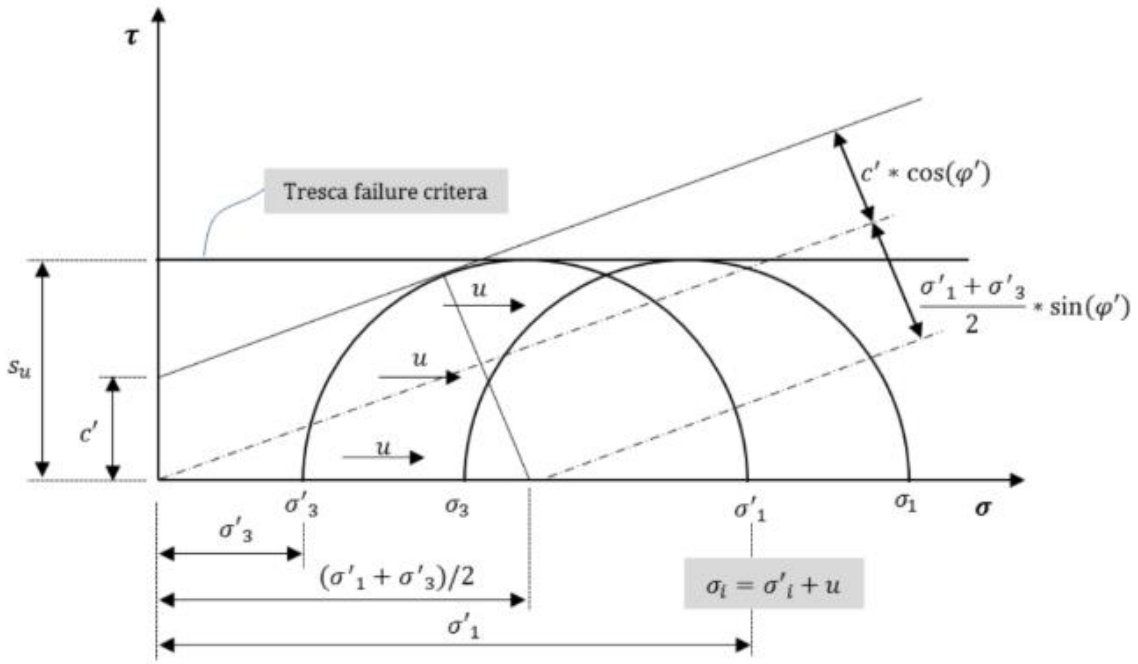

Figure 16: Mohr's circle of stress and Tresca failure criteria implemented.

3.2 Effect of anisotropy on shear strength

Anisotropy means that a material has properties that vary in different directions. In geotechnics, anisotropy in clays will imply that physical properties such as stiffness and strength, depends on the direction in which the material is loaded (Thakur et.al, 2014).

Low plastic clays, such as Norwegians ones with brittle properties, generally exhibit greater anisotropy than high- plastic clays. Therefore, it is especially important to consider the shear strength anisotropy so that available shear strength along critical sliding surface can be modelled correctly. The anisotropic state load in a slope is outlined in figure 17 as an active, direct, and passive condition. In the figure this is shown as shear strength directions in earth elements along a sliding surface.

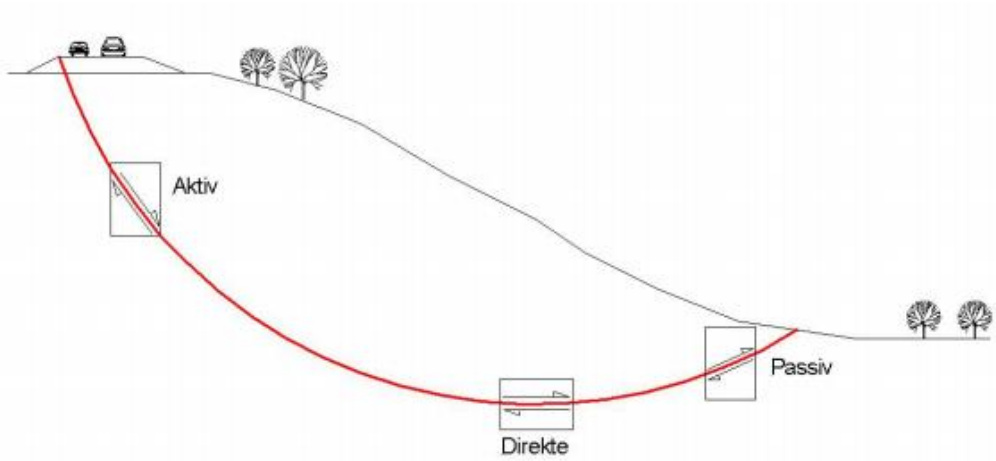

Figure 17: Illustration of anisotropic stress state on a slope, with a road filling on top (Fauskerud et al,2012).

Empirical correlations indicate that direct shear strength su_D lies somewhere between active and passive shear strength (suA > suD > suP) (Nordal, 2018). The following conditions (equations 2, 3, 4) underline how undrained shear strength varies with the loading direction and highlights the importance of taking into account the anisotropy conditions for slope stability.

$$suA = 0.3 \times \sigma vo' \quad (2)$$

$$suD = 0.2 \times \sigma vo' \quad (3)$$

$$suP = 0.1 \times \sigma vo' \quad (4)$$

3.3 General Slope stability

To access the stability of a slope, the factor of safety is established. The factor, given in equation 1.1, is the ration between stabilizing and driving forces, where a number larger than 1.0 represents a stable slope and values below 1.0 represents an unstable slope (Emdal et al., 2014).

F= Stabilizing Forces / Driving Forces (5)

The stabilizing forces can consist both of internal material properties, such as friction between the grains or cohesion. External measures, such as counter fills or unloading by removing material from the top of the slope may also contribute to the stabilizing forces. The driving forces are mainly gravity driven, water pressures or external loads. Different methods may be used to calculate the factor of safety i.e. probabilistic approaches or limit equilibrium methods. One of the most common material models applied for soils, is the Mohr Coulomb model. The Mohr- Coulomb failure live governs the strength of the material and is given by the equation below.

$$\tau_f = c + \sigma' tan\varphi = (a + \sigma')tan\varphi \quad (6)$$

Where,

τ_f = Shear strength

c = cohesion

σ' = effective normal stresses

a = attraction

tanφ = friction coefficient

3.4 Theoretical analysis of Plaxis software

Plaxis is a finite element analysis software developed by Plaxis Company. Compared with other Finite Element analysis software as ANSYS Abaqus etc., Plaxis is the one designed for geotechnical problems, soil, or rock slope. Plaxis set different soil models as Mohr-Coulomb, Advanced soil model, Hardening soil model, NGI-ADP model, and user designed model. The soil test option is a convenient tool to study soil behavior.

3.4.1Safety analysis in Plaxis

Safety analysis uses a method called c- φ reduction. It's a method in which, strength of the soil material will be reduced with a factor ΣMsf until either failure is reached for a stable value of ΣMsf, or the maximum number of a calculation step is reached. The main rule for this reduction is the following:

$$\Sigma Msf = \tan(\varphi' input) \div \tan(\varphi' reduced) = c' input \div c' reduced \qquad (7)$$

Basically, Plaxis will reduce the strength incrementally until the point where the soil body collapse is reached. Value of ΣMsf at failure gives the final factor of safety.

3.4.2Mohr- Coulomb model analysis

The Mohr Coulomb model represents a "first order" approximation of soil or rock behavior. It is recommended to use this model for a first analysis of the problem considered. For each layer one estimates a constant average stiffness or a stiffness that increases linearly with depth. Due to this constant stiffness, computations tend to be relatively fast and one obtains a first estimate of deformations. In the table below, the five input parameters for this model are presented.

E	Young's Modulus	Kn/m^2
v	Poisson's ratio	-
c	Cohesion	Kn/m^2
φ	Friction angle	^{o}
ψ	Dilatancy angle	^{o}

Table 2: Parameters in Mohr Coulomb analysis

In the Mohr-Coulomb model, undrained behavior could be modelled by setting the friction angle φ equal to zero and the cohesion c to cu, the undrained shear strength. However, when using this approach only the undrained shear strength is considered. Regarding the stiffness of

the soil, still the drained situation is assumed. Also, this model does not take into account the process of consolidation, and therefore with this approach caution is required for loads of longer duration (Plaxis, 2018).

3.4.3NGI-ADP model analysis

The NGI-ADP model may be used for capacity, deformation and soil-structure interaction analyses involving undrained loading of clay. The basis of the material model is:

- A yield criterion based on an approximated Tresca criterion.
- Input parameters for undrained shear strength for three different stress states (Active, Direct, Passive) (see in chapter 3.2).
- Isotropic elasticity, given by the unloading/reloading shear modulus, Gur.
- Elliptical interpolation functions for plastic failure strains and for shear strengths in arbitrary stress states.

The table below summarizes the input parameters used in ADP models. Further on this task an NGI-ADP model is used for stability calculations in Sørkjosen.

Parameter	Symbol	Description	Unit
NGI-ADP MODEL	G_{ur}/s_u^A	Ratio unloading reloading shear modulus over plane strain active shear strength	[-]
	γ_f^C	Shear strain at failure in triaxial compression	%
	γ_f^E	Shear strain at failure in triaxial extension	%
	γ_f^{DSS}	Shear strain at failure in direct simple shear	%
	s_u^A.ref	Reference plane strain active shear strength	kN/m^2
	y_{ref}	Reference depth	m
	s_u^A.inc	Increase of shear strength with depth	$(kN/m^2)/m$
	s_u^P/ s_u^A	Ratio of plane strain passive shear strength over (plain strain) active shear strength	[-]
	τ_0/ s_u^A	Initial mobilisation	[-]
	s_u^{DSS}/ s_u^A	Ratio of direct simple shear strength over (plane strain) active shear strength	[-]
	v	Poisson's ratio	[-]
	v_u	Poisson's ratio undrained	[-]

Table 3: Parameters in ADP analysis

3.4.4Undrained effective stress analysis (Undrained B)

In Plaxis it is possible to define undrained behavior in an effective stress analysis using effective model parameters. This is achieved by identifying the type of material behavior (Drainage type) of a soil layer as Undrained A or Undrained B. In this report the clay layer has been specified as Undrained B behavior.

For undrained soil layers with a known undrained shear strength profile, Plaxis offers the Undrained B model with direct input of the undrained shear strength i.e. setting the friction angle to zero and the cohesion equal to the undrained shear strength ($\varphi=\varphi u=0$; $c = su$). Also, in this case, distinction is made between pore pressures and effective stresses. Although the pore pressures and effective stress path may not be fully correct, the resulting undrained shear strength is not affected since it is directly specified as an input parameter.

The option to perform an undrained effective stress analysis with undrained strength parameters is only available for the Mohr-Coulomb model, the Hardening soil model, the HS small model and the NGI-ADP model.

4. Case study: Sørkjosen landslide

Landslides along Norwegian fjords occur periodically and are a threat to coastal communities. Analysis of past landslide events gives important information on factors contributing to an initiating failure, mass propagation as well as tsunamigenic potential. The aim is to reduce the risk for new landslides.

A shoreline landslide of between 1,1 and 1,4 million m3 took place close to the village Sorkjosen in Northern Norway during the night of the 9th to the 10th May 2015 (see location in figure 18 and 19). The shoreline was destroyed over more than one kilometer. In the north a warehouse slumped into the sea whereas in the south a pier sank in the fjord, destroying a harbor. A small tsunami was triggered in the fjord. No casualties were encountered, but the landslide closed the main road, E6, connecting North and South Norway. After the landslide, the traffic had to take 700 km detour through Finland to get across.

In the next chapters information regarding this landslide will be presented.

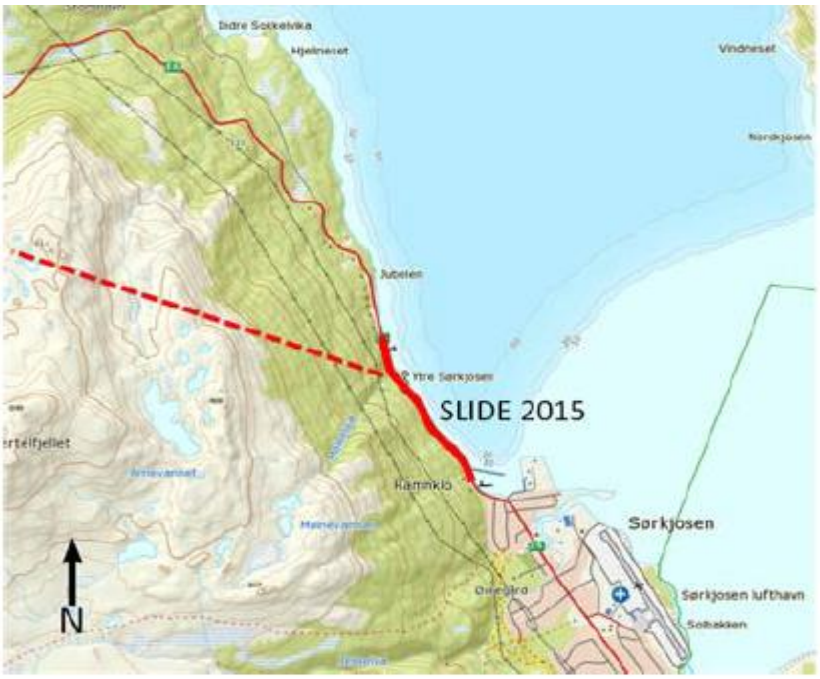

Figure 18: The 2015 slide sent the shoreline marked by a solid line into the fjord. The dotted line was a rock tunnel under construction.

4.1 Geology of the area

Sørkjosen is a village located in Troms and Finmark county. The village is located along the shores of the Reisafjord. For approx. 10,000 years ago, the entire Sørkjosen area was below sea level and marine deposits (i.e. clay and silt) became bottom layers. The rise and fall in relative sea level eventually led to a northern progression of the Reis delta and powerful sand deposits were deposited over clay at the mouth of the Reisa river. Sørkjosen was slowly formed because of Reisa's

Figure 19: Sørkjosen area.

transport of sediments and loads combined with land elevation. The stratification at Sørkjosen is illustrated with schematic sections in Figure 20. Based on results from exploration and expected geological deposition history in the area, high sand deposits can be expected over a continuous clay layer in the delta area. To the west and east along the valley sides there will be shallower clay deposits and to the bedrock.

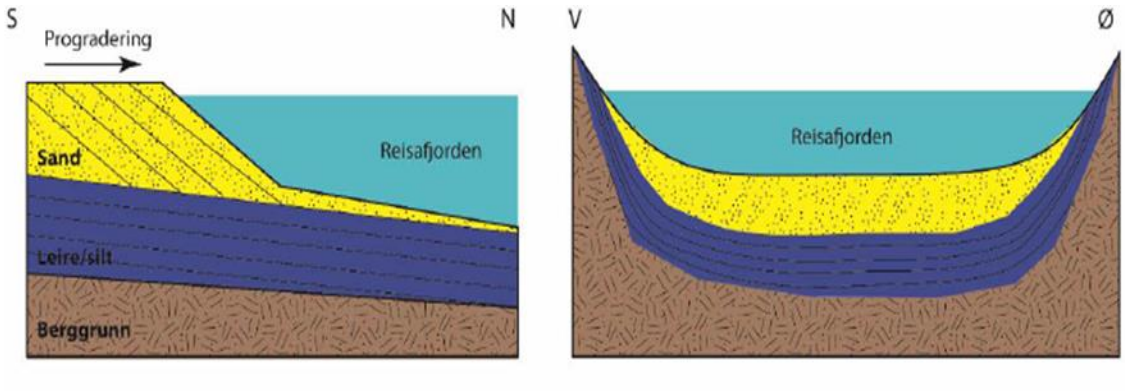

Figure 20: Schematic illustration of the Reis delta at Sørkjosen in two vertical sections, one from south to north (left) and one from west to east (right). N.B: Not in scale.

Simply put, the local loads can be divided into three layers. At the top lies a layer of loose to medium firmly stored sand / silt (Layer 1), followed by a layer of clay / silty clay that is occasionally brittle (Layer 2). Below this lies a fixed layer of the supposed bedrock (Layer 3). Layer thicknesses and depths of rock vary considerably from the area to the South up to the area in the North.

4.1.1Soil conditions

Soil investigations were carried out prior to and after the landslide both on and offshore. The investigations included total soundings, cone penetration tests (CPTU), piezometers, soil sampling and laboratory investigations. Results show that soil deposits are dominated by loose to medium dense sand and silt over clay and silty clay on a discontinuous layer of moraine upon bedrock. The clay was partly sensitive.

Figure 21 presents undrained shear strength interpretations in the clay based on CPTU results and laboratory testing. The sounding on figure 21 was carried out in the fjord inside the evacuated landslide scar near the pier at a water depth of 7 meters. Before the landslide event, this location was covered by 14 meters of sand and rock fill up to an elevation of +4 m.a.s.l. In the sounding on figure 21 the top of the clay has an undrained shear strength varying between 25 to 35 kpa and is covered by sand and debris from the landslide. Table 4 in chapter 4.6 summarizes geotechnical strength parameters based on the study group's interpretations of pressure probes (CPTUs) and laboratory experiments, supplemented with experience values from similar basic conditions.

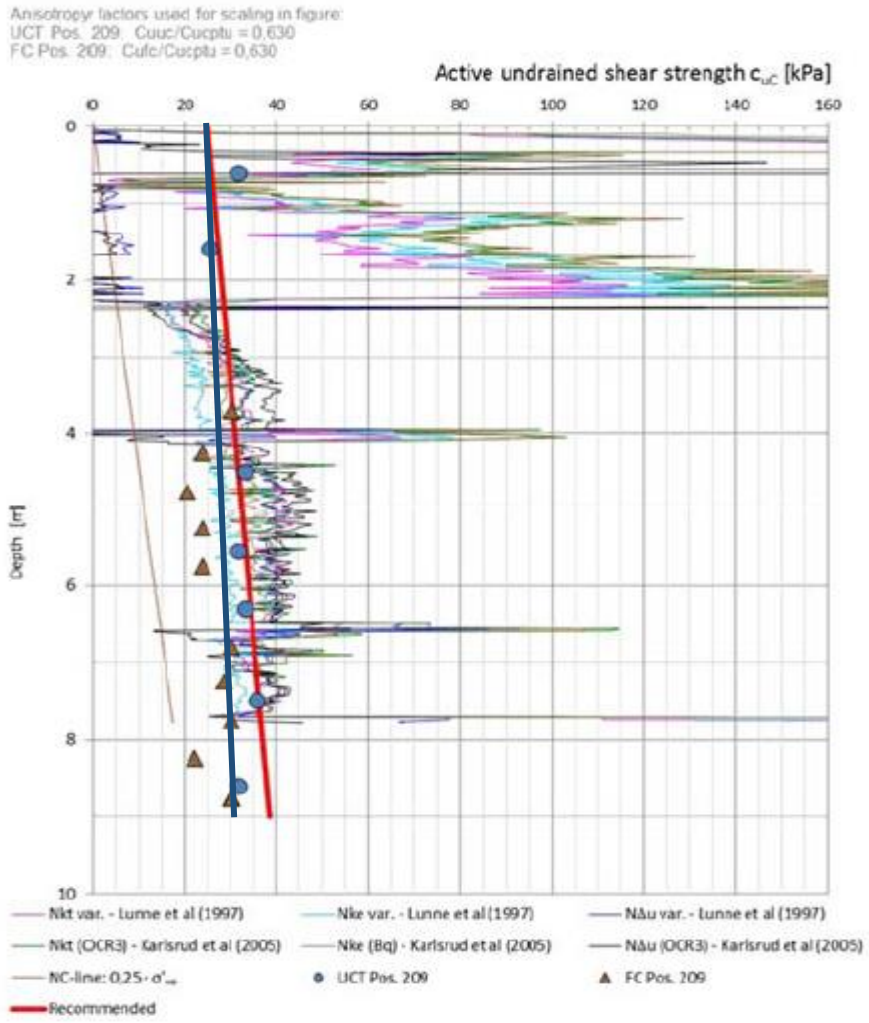

Figure 21: Undrained active shear strength results from soil investigations performed after the slide within the evacuated scar (modified in order to include the su used in this paper (blue line)). The failure surface corresponds to the top of the clay layer now covered by landslide debris. (Nordal S, L'Heureux J. 2016)

In Figure 21 the deep blue line is the undrained shear strength used in this thesis for the varying su calculations in chapter 5.3. The inclination is less steep (lower su,increment was used in plaxis software). The reason might be the different material models used in this paper and in the investigation report (Nordal S, L'Heureux J. 2016). NGI-ADP material model used in the investigation report, takes into account the anisotropy of the soil while Mohr Coulomb, used in this paper, assumes isotropic conditions.

4.2 Bathymetry

Most of the landslide on May 10th took place under water. A survey of the seabed was necessary to see the extent and other features of the landslide. Figure 22 shows a relatively smooth seabed with a regular wavy pattern in the surface. The pattern is due to migrating sand waves formed by the deposition process. The west side of the area, where the landslide took place in 2015, shows no signs of any previous landslide activity in 2006 (and 2011).

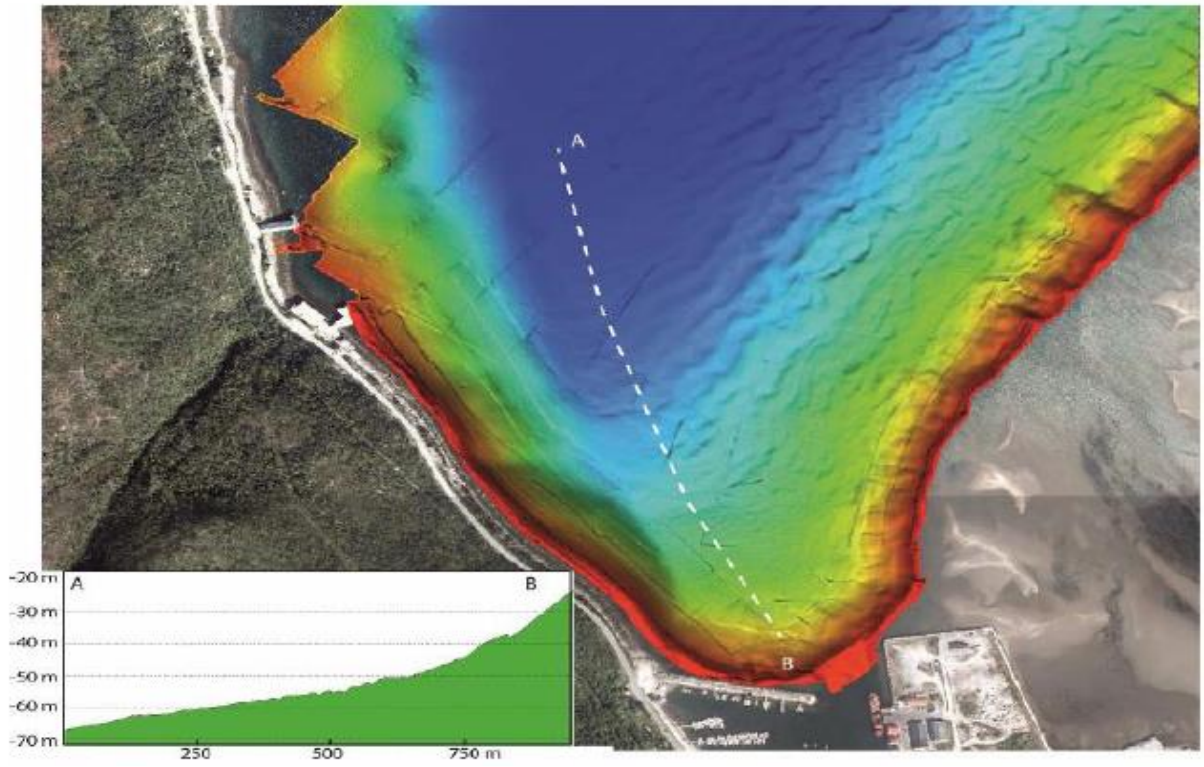

Figure 22: Bathymetry from 2006 shows the seabed before the landslide (investigation report (Nordal.S, L'Heureux.J, Skotheim. A, 2016)).

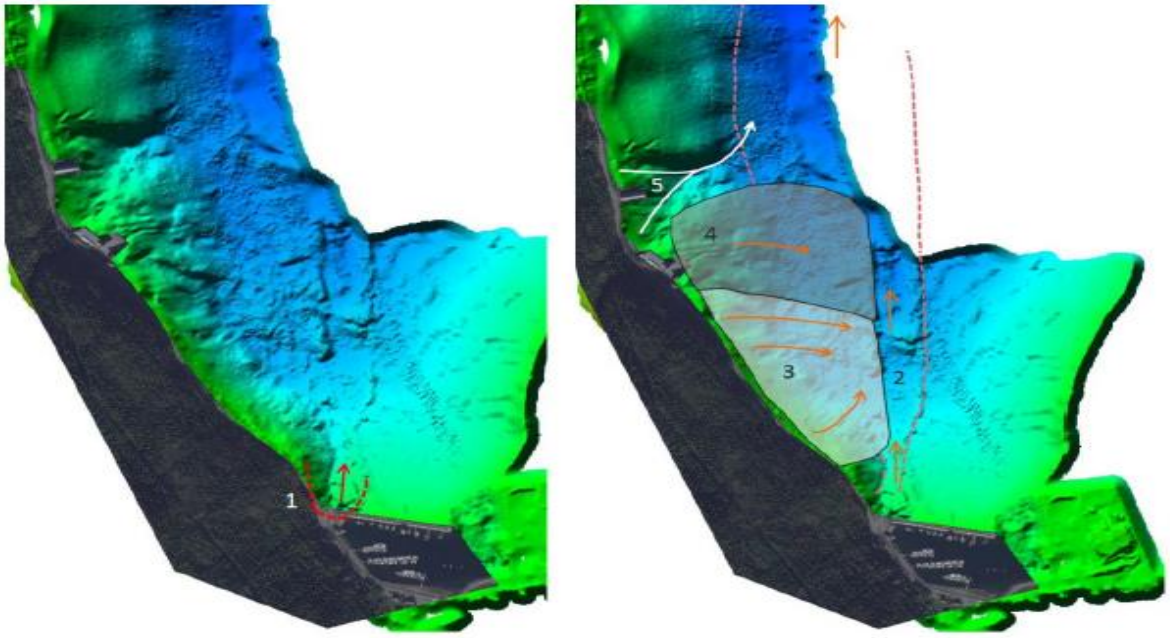

Figure 23: Bathymetry after the landslide with interpretation of the a) initial landslide b) secondary landslide (investigation report (Nordal.S, L'Heureux.J, Skotheim. A, 2016)).

Interpreting high resolution bathymetry on screen where one can shade and rotate to the desired viewing angle shows with great certainty that a deep landslide first emerged at the pier as illustrated in Figure 23a. The direction of movement of these landslides is evident and the traces of them disappear into other landslides, which came from the shoreline along E6, see phase 2 in Figure 23b. The subsequent secondary landslides are numbered 3, 4 and 5 in Figure 23b. The last of the secondary landslides occurred in Jubelen at the tunnel cut, phase 5 in Figure 23b. While the landslides towards the pier went about 20 meters into the seabed and into the clay, the landslides at Jubelen went shallow, approx. 5 meters.

The masses from the landslide were dominated by loose to medium sand and silt deposits. Due to the steep sea floor and large altitude differences outside the pier, the landslides gained great speed throughout the fjord along shore. The landslides took a footing on the submarine slopes along the E6 from the pier and all the way to Jubelen. Bathymetry data after the landslide shows traces of the strong erosion process associated with the movement of the masses from the area at the pier (Figure 24).

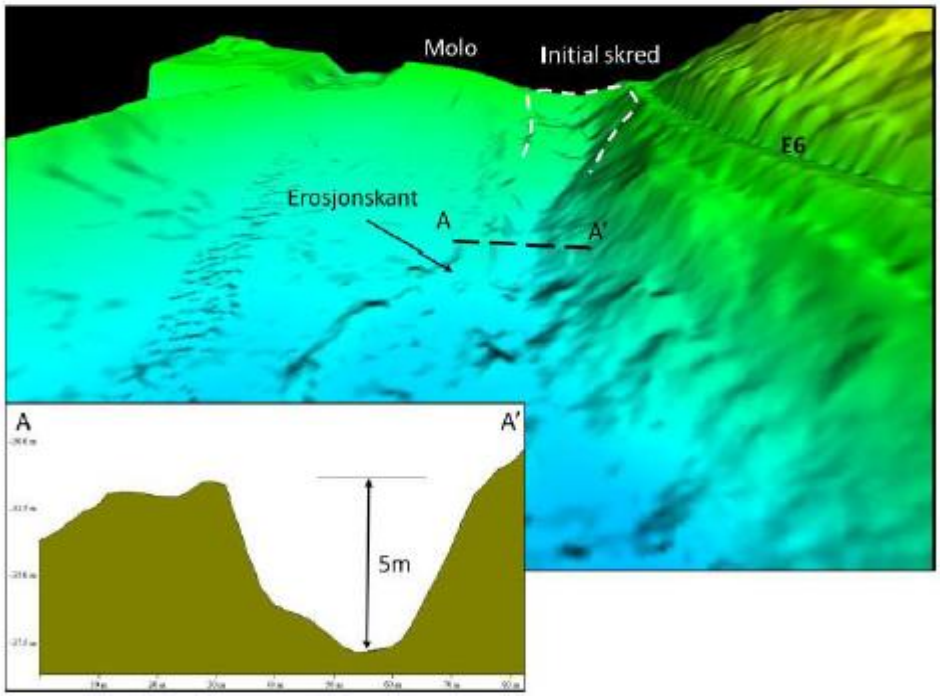

Figure 24: 3D illustration of bathymetry after avalanche with interpretation of the erosion below the initial landslide (investigation report (Nordal.S, L'Heureux.J, Skotheim. A, 2016)).

4.3 Precipitation and tide

Heavy rainfall was observed in the afternoon and evening on May 9, the day before the avalanche. There was also a significant snow melt and witnesses tell of large amounts of water in all ditches and culverts. About 25 mm of precipitation was recorded as rain at Sørkjosen Airport between 07:00 of the 9th of May and 07:00 of the 10th of May, Figure 22. The last four days before the avalanche, there was an estimated snow melt of 15 to 20 mm / day from model height 380 m. These conditions led to increasing water flow in streams and small rivers. In total, snowmelt and precipitation provide an equivalent rainfall for May 10 of 40 to 45 mm / d.

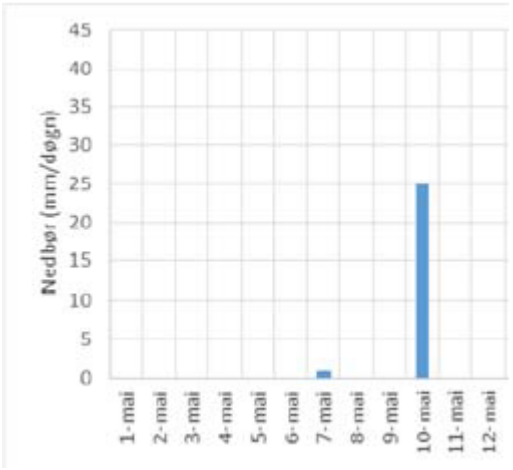

Figure 25: Measured rainfall at Sørkjosen Airport in the last 24 hours before 7am of the 10th of May. (source: eklima.no). Significant snowmelt should be also considered to fully understand the effect of this rain.

NVE (Norwegian Water Resources and Energy Directorate) notified on May 9, 2015 at. 09.52 danger of flooding with level of care 2 in Troms and Finnmark. The avalanche occurred after the low tide, which was 43pprox.. at midnight. In Sørkjosen there is a tidal difference of 2 – 3 meters. The avalanche occurred 43pprox.. kl. 02.40 night to 10 May with an observed water level of 39 cm below normal 1954. Low tide occurred at. 00.00 night to 10 May with an observed water level of 99 cm below normal zero 1954, see Figure 11. Naval chart zero (LAT) is set at 182 cm below normal zero 1954. Thus, it was not uncommonly low tide in the time before the avalanche.

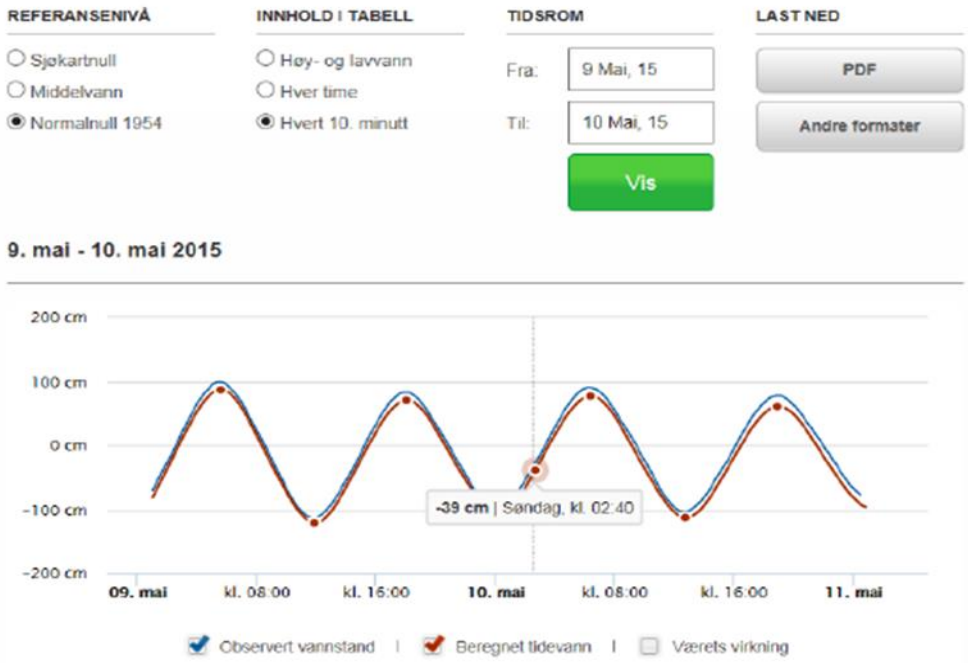

Figure 26: Calculated and observed tides for Sørkjosen (from Sehavnivå.no).

4.4 Construction work with timeline

Work was underway on E6 during the E6 Langslett – Sørkjosen project in the months before the avalanche. The project was to expand and upgrade the road from Sørkjosen with a new tunnel from Jubelen to Langslett on the other side of Sørkjosenfjellet. Work on the section in question was divided into two execution contracts. Målselv Maskin was awarded the contract on the road today (T01) in December 2013, while the Spanish contractor Obras Subterraneas (Ossa) was awarded the contract on the tunnel 28.08.2014 (T02).

The slide took place on May 10, 2015. On the same day and in the days before the event, heavy rainfall took place in the mountains between the pier and Jubelen. The drainage provided small amounts of rock and none of it was tipped into the sea on the stretch but run out of area. The amounts of water for flushing may seem large but are vanishingly small compared to what a rainfall would provide in the same area. There is little evidence that this activity has had any impact on landslides.

The last blast in the tunnel was blown up on March 30, over a month before the landslide and it seems unreasonable that the tunnel operation may have had an impact on the landslide. When information was received that a water had dried up on the mountain, it was suggested that the blasts could have opened cracks / waterways in the rock / mountain so that water access to the slide area had increased over time. However, little water was recorded in the blasted tunnel, and from the terrain and rock formations the study group concluded that increased water access from new and or expanded cracks / waterways must be insignificant and of no significance to the slide.

A plastic pipe for water from the tunnel was laid over the road in Jubelen on February 5, 2015 and on the bottom in the order of 50 meters into the sea about 3 months before the slide. The pipe came from a closed sludge separation chamber and did not carry much water, probably not during the heavy rainfall on Saturday afternoon on May 9.

A new filling was added to the pier through expansion of the old one, Figure 24. It was laid out in two layers during the period from October 1 to November 21, 2014. Damage to the plastic ring on the outside of the filling was discovered on January 5, 2015 and immediately rectified. This is a sign of local instability.

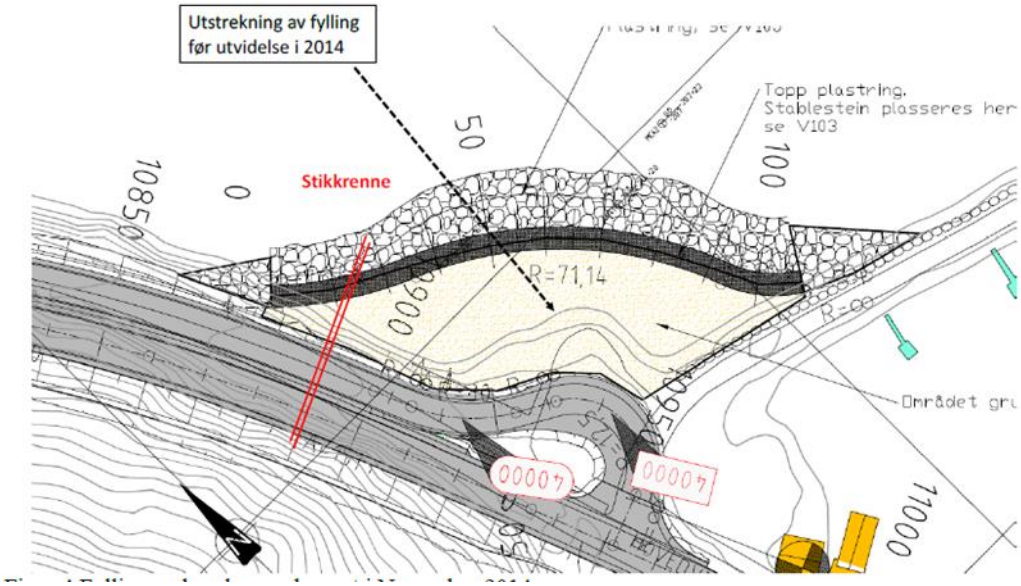

Figure 27: Filling at the pier as built in November 2014 (Nordal.S, L'Heureux.J, Skotheim. A, 2016)

There was significant rainfall in the afternoon of May 9 and witnesses told of large amounts of water in the mountain cut, in the ditches along this and in the ditches under the road. The cuttings were laid between October 13 and November 14, 2014. A cutting was laid through the road 45 approx. at el. 10890 and went out into the sea through the new filling. Figure 27 shows the plug run after the landslide. The extent of the old filling at the foot of the pier is shown in the cones in Figure 28.

Figure 28: A photo from the seaside shortly after the landslide. Shows the northern part of the area where the pier reached land and the cuttings that passed through the road and the landfill. (Photo: Norut, ISBN 978-82-7492-305-8 report).

4.5 Load conditions at the pier

The pier at Sørkjosen was built in 1977. In autumn 2014, a landfill was laid on the pier at the part for exits to the local road and the marina parking lot, using rocks from the mountainside further north along the E6. This work was completed in November 2014. Orthophotos from the molo area show that there have been fillings in various phases in this area during the period 1994-2014 (Figure 29). An overview of the filling at the parking lot is presented in Figure 30. The top of the filling at the parking lot is on the cot 46pprox.. 4 m, while the outer part of the pier to the east lies at the foot 3m.

Figure 29: Orthophotos of the pier at Sørkjosen in the period 1994-2015 illustrate filling in over time, as well as the situation after the slide. (Nordal.S, L'Heureux.J, Skotheim. A, 2016)

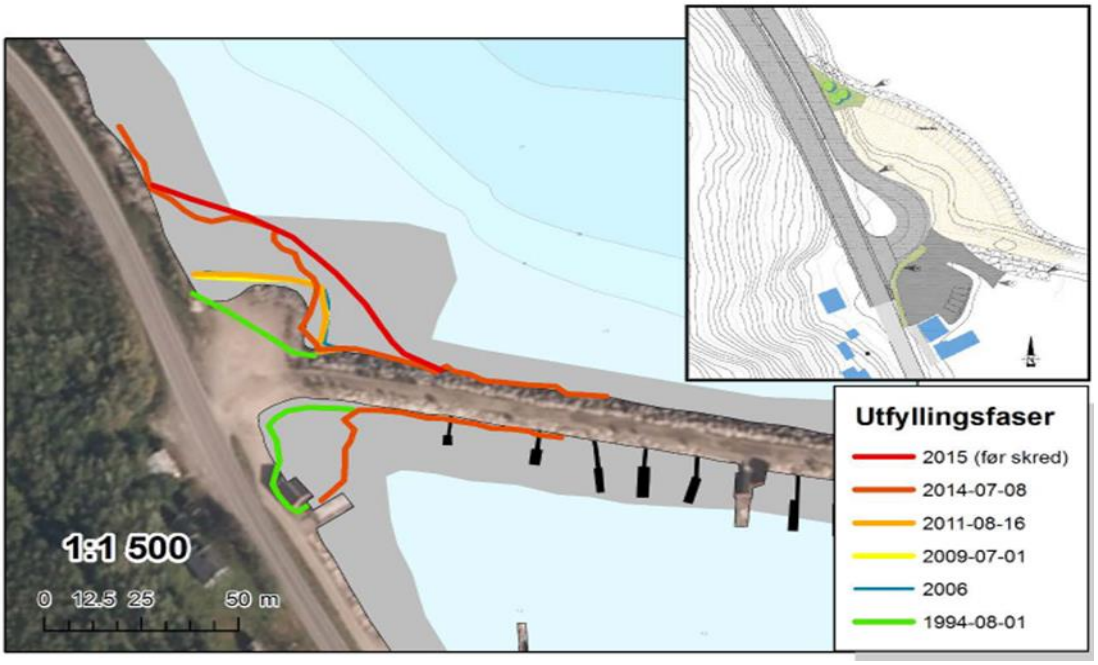

Figure 30: Overview of the filling at the pier at Sørkjosen over time. The drawing at the top right shows the completed completion in November 2014 and until the landslide on 10 May 2015.

4.6 Strength parameters for stability assessments at the pier

The investigation report of the landslide event is used to determine the strength parameters for the area (Nordal.S, L'Heureux.J, Skotheim. A, 2016). Stability calculations have been performed at the pier in profile 31, as shown in appendix 1.

Layer	1	2	3
Soil	Sand/silt	Clay	Bedrock
Friction angle φ (^{0})	33-38	25-30	35-40
Attraction a (kpa)	0 – 5	10-20	10-20
Unit weight γ (kN/m3)	19 – 19.5	19-20	18-20

Undrained shear strength sua	-	sua= 30-35 kpa	-

Table 4: Strength parameters for profile 31.

5. Calculations

In the investigation report after the landslide (Nordal.S, L'Heureux.J, Skotheim. A, 2016) the stability calculations were performed with Plaxis software and NGI-ADP as material model (with undrained shear strength varying with depth). In the next chapter stability has been recalculated with the Mohr-Coulomb criterion as material model. All the stability calculations have been performed in profile 31(appendix 1).

5.1 Plaxis parameters

	Name	Fill	Sand-Silt	Clay	Bedrock	Units
Material model	model	Mohr-Coulomb	Mohr Coulomb	Mohr-Coulomb	Linear elastic	-
Material type	type	Drained	Drained	Undrained B	Drained	-
Unit weight	(γ_{sat}=γ_{unsat})	20	19	19	γunsat= 27 γsat= -	Kn/m^3
Young's modulus (constant)	E	10000	10000	8000	1,00E+8	kpa
Poisson's Ratio	v	0.33	0.33	0.33	0.2	-
Cohesion	c	20	0	0	-	kpa
Friction angle	φ	40	33	φu = 0	-	^{0}
Dilatancy	ψ	0	0	0	-	^{0}
Undrained shear strength	su	-	-	33 (constant)	-	kpa
Color in Plaxis model		Purple	Light blue	Green	Light yellow	-

Table 5: Geotechnical parameters used in plaxis calculations.

In order to simulate the conditions at the time of the slide in May 2015 the external water was lowered by 2 m to fit with the tidal level just before the slide. Also, the pore pressure changes at depth had almost no effect since here the undrained strength of the clay controlled the incident.

.

5.1.1Modelling of undrained shear strength (su)

The shear strength definition is based on the individual analysis tool used. For some software, the shear strength of a soil is described by interpolation between given strength profiles. If a strength profile is known at the top of a slope and another at the foot of the same slope, the program will automatically generate a strength profile for the soil layer between them.

In the built-in model for Plaxis used in this paper, Mohr-Coulomb and NGI-ADP, specify the strength parameters for undrained case according to a height reference, yref. So, for a selected material the shear strength increases with height reference and not with depth. Different approaches have been made to describe the shear strength conditions in Plaxis.

One approach is looking at the clay layer as completely homogeneous. A characteristic shear strength is, therefore, chosen to be valid for the entire material, regardless of depth (chapter 5.2).

Another method has been to divide the clay layer into two slices (two clay layers with same properties except the shear strength profile). At the top of the layer (suA.ref.) is constant and the other layer has an increase per depth (suA, inc.), while the reference point (yref.) varies

Finally, the third technique was to have a varying shear strength in both clay layers. In this way a realistic shear strength profile was achieved (chapter 5.3).

5.2 Calculations with homogeneous clay layer

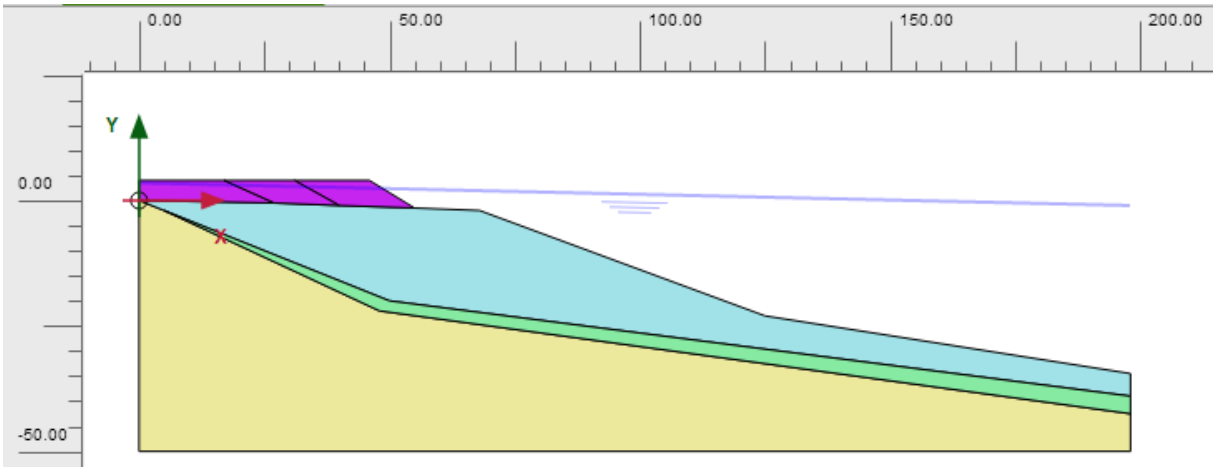

Figure 31: Plaxis model (profile 31)

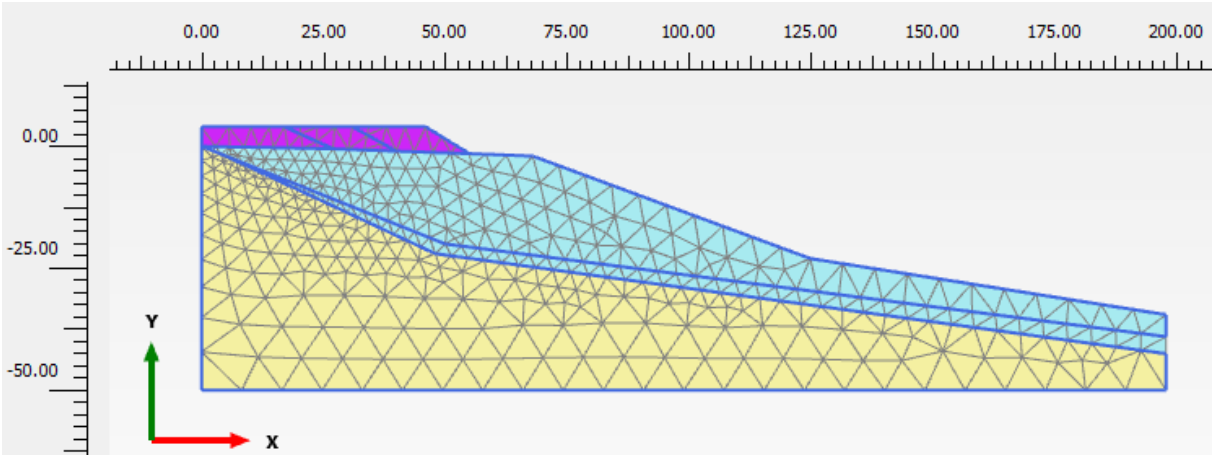

Figure 32: Model from Plaxis for homogeneous clay layer. The figure shows divided mesh (fine= 0.04002), generated 767 elements and 6291 nodes.

Calculation phases:

1) Initial phase with no filling.
2) Filling level 1 (1994)
3) Phase with c- φ reduction to access safety
4) Filling level 2 (2006)
5) Phase with c- φ reduction to access safety
6) Filling level 3 (2015)
7) Phase with c- φ reduction to access safety

	su= 33 kpa
FoS Before 2015's fill	1.072
FoS After 2015's fill	1.011

Table 6: Results for homogeneous clay layer.

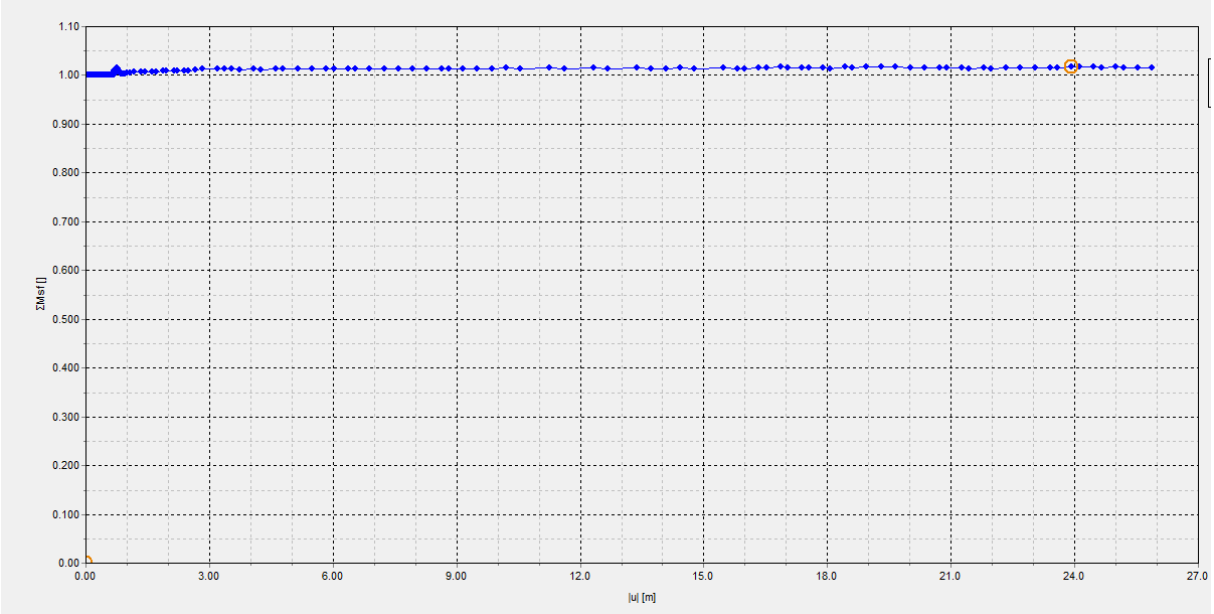

Figure 33: Safety factor obtained for the constant su (table 6).

5.3 Calculations with varying undrained shear strength

A new model has been created with two clay layers (same properties with different shear strength profiles). The goal was to obtain a more realistic approach by dividing the clay into two units (light and dark green layers).

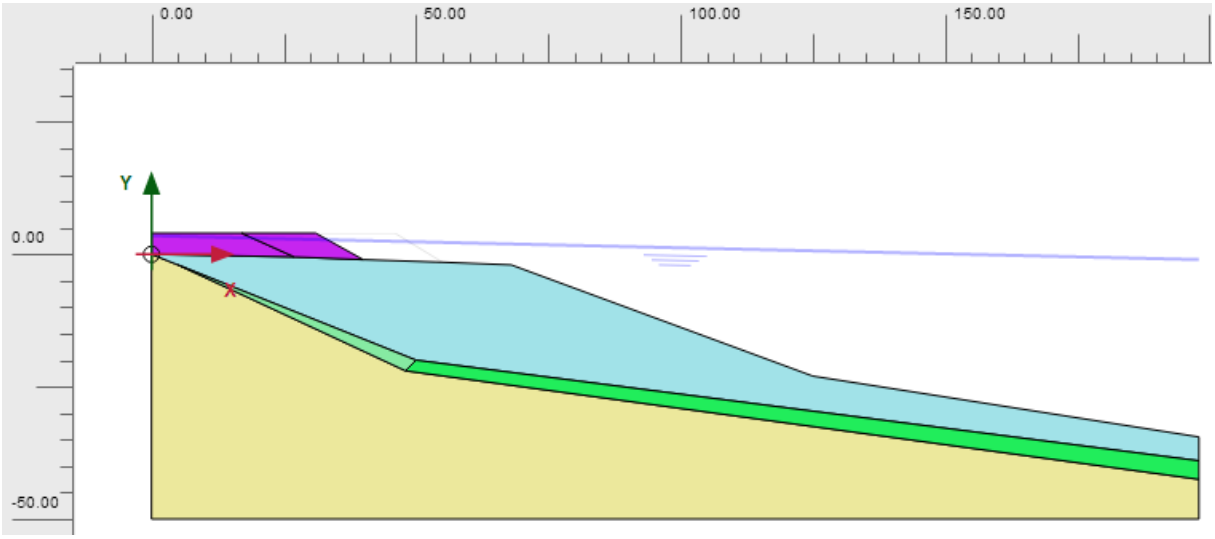

Figure 34: Plaxis model for two clay layers.

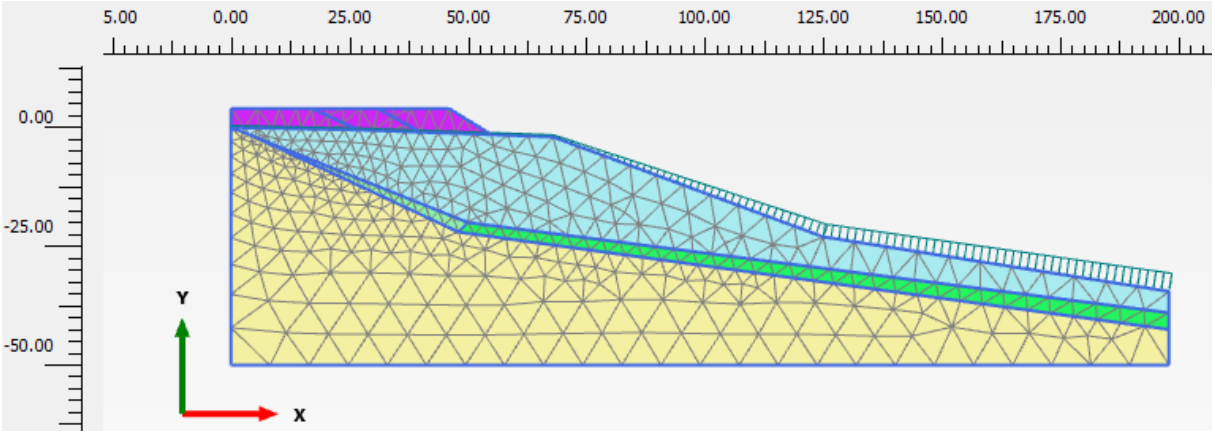

Figure 35: Model from Plaxis for two clay layers. The figure shows divided mesh (fine= 0.04002), generated 767 elements and 6291 nodes.

Calculation phases:

1) Initial phase with no filling.
2) Filling level 1 (1994)
3) Phase with c- φ reduction to access safety
4) Filling level 2 (2006)
5) Phase with c- φ reduction to access safety

6) Filling level 3 (2015)
7) Phase with c- φ reduction to access safety

5.3.1Calculations for varying su for lower clay layer

The table below summarizes the parameters and the safety factors obtained by using the Mohr-Coulomb criterion with varying undrained shear strength.

First, the higher layer had a constant su and the lower clay layer had a varying one.

	Higher clay layer (light green)	Lower clay layer (dark green)
Undrained shear strength	su= 34 kpa	Su,ref = 34 kpa Suincr = -0.05 kpa Yref = 22 m
FoS Before 2015's fill	1.058	
FoS After 2015's fill	1.005	

Table 7: Results for varying undrained shear strength.

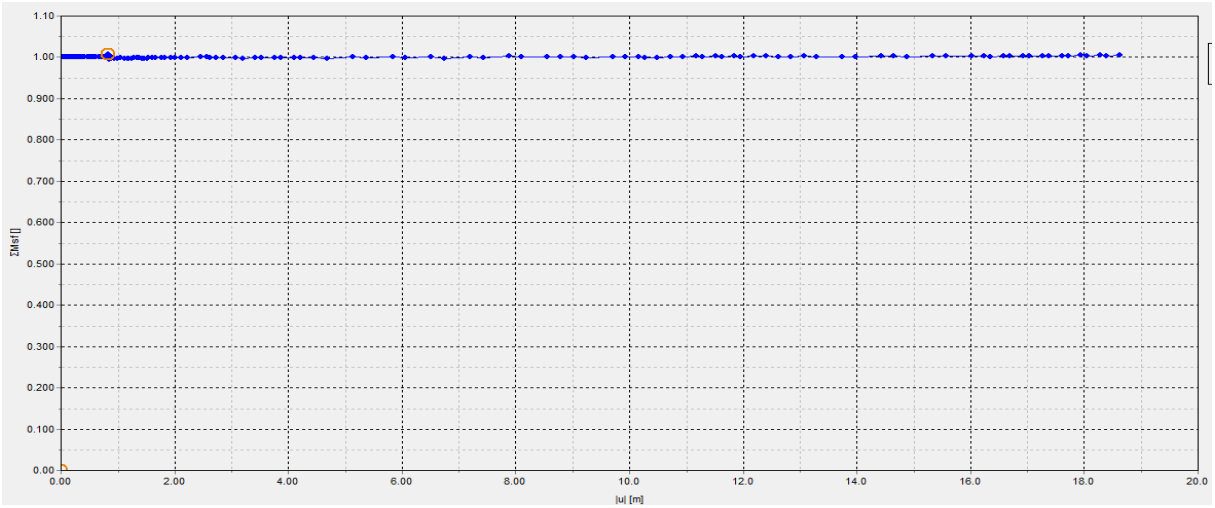

Figure 36: Safety factor obtained for varying su (table 7)

5.3.2Calculations for varying su for both clay layers

	Higher clay layer (light green)	Lower clay layer (dark green)
Undrained shear strength	su, ref= 25 kpa suincr. = 0.45 kpa yref= 0 m	Su,ref = 34.9 kpa Suincr = -0.05 kpa yref = 22 m
FoS Before 2015's fill	1.043	
FoS After 2015's fill	1.003	

Table 8: Results for varying undrained shear strength.

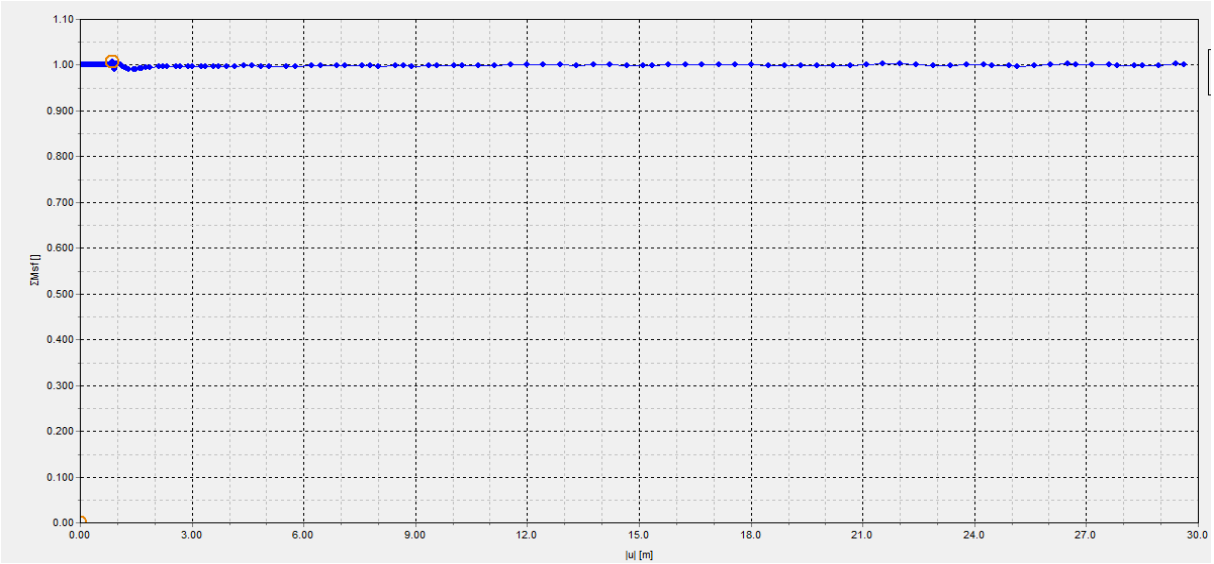

Figure 37: Safety factor obtained for varying su (table 8)

6. Discussion of the results

As mentioned earlier in the thesis, several landslides in the shoreline have occurred near weak layers. To what degree layers of sensitive clay exists in Sørkjosen requires further investigation.

Also, the filling in the pier area was placed disadvantageously in relation to several factors. The slope near the filling is very steep and more susceptible to erosion.

Also, all the calculations in the previous chapter were performed with Mohr Coulomb as material model. In the investigation report after the landslide in 2015, the NGI-ADP model was used (Nordal.S, L'Heureux.J, Skotheim. A, 2016). The failure mechanism from this report is showed in figure 38. Comments will be made in the following chapters comparing the results for the failure mechanism figure below and the mechanism from the calculations of the previous chapters.

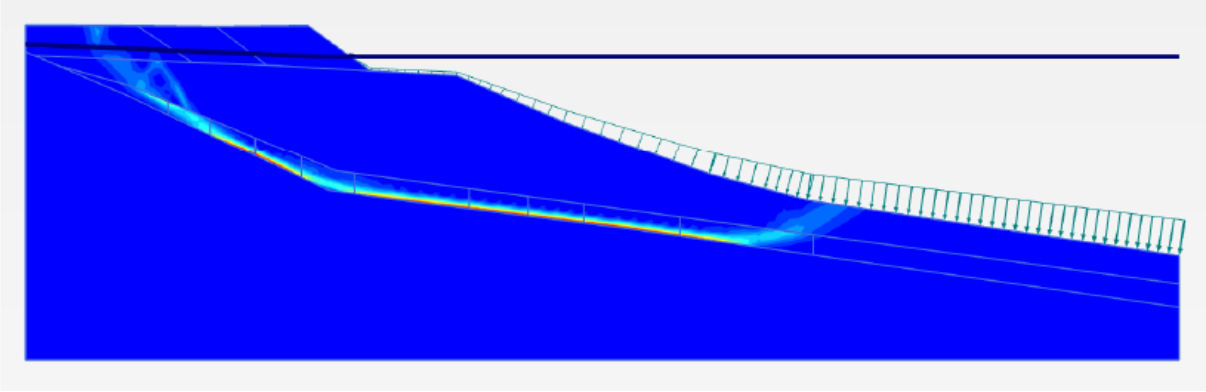

Figure 38: Failure mechanism from the investigation report after the incident. (Nordal.S, L'Heureux.J, Skotheim. A, 2016).

6.1 Results from constant su

A simplified model, where the shear strength is the same for the whole clay layer was generated. A characteristic value equal to 33 kpa was chosen based on the shear strength of about 22m with clay under the filling.

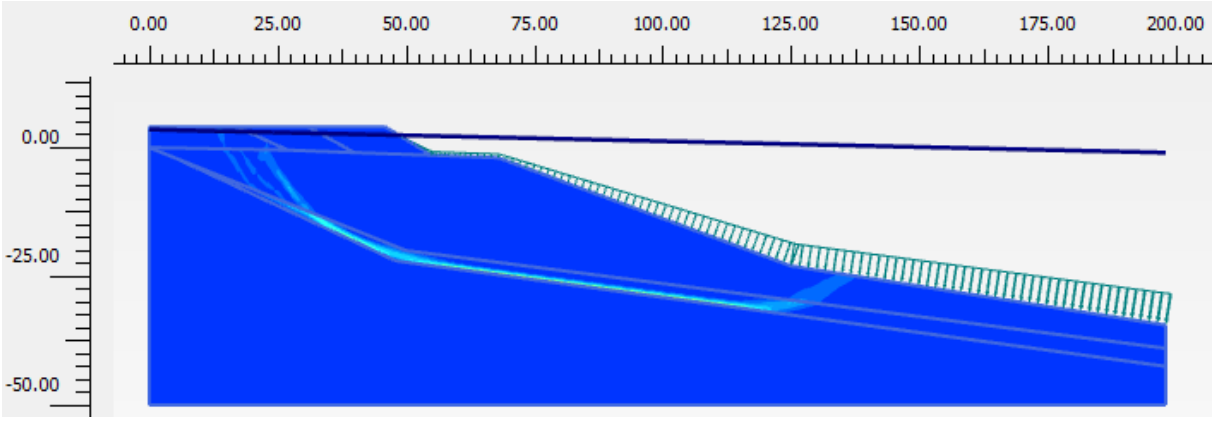

Figure 39: Failure mechanism for constant su equal to 33 kpa.

The shape of the failure mechanism corresponds well with the one in figure 38. NGI-ADP model is giving larger incremental strains in the slip surface though. This is expected because NGI-ADP is an anisotropic undrained shear strength model while MC assumes isotropic conditions. In other words, NGI-ADP uses different shear strengths along various failure surfaces. In the event where there is a smaller shear stress in a given orientation the soil will reach failure rapidly and therefore large strains will occur.

6.2 Results from varying su

One of the purposes for this approach was to get an idea of how the shear strength conditions may have been when the landslide was triggered. Undrained shear strength varying with depth is a more realistic and practical technique.

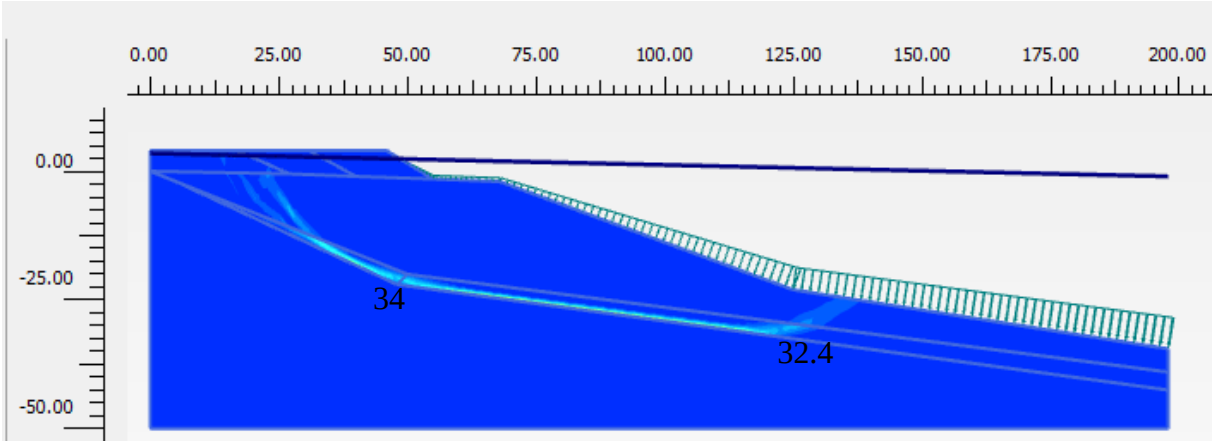

Figure 40: Failure mechanism for varying su in the lower clay layer. The undrained shear strength values are presented on the failure surface (unit kpa).

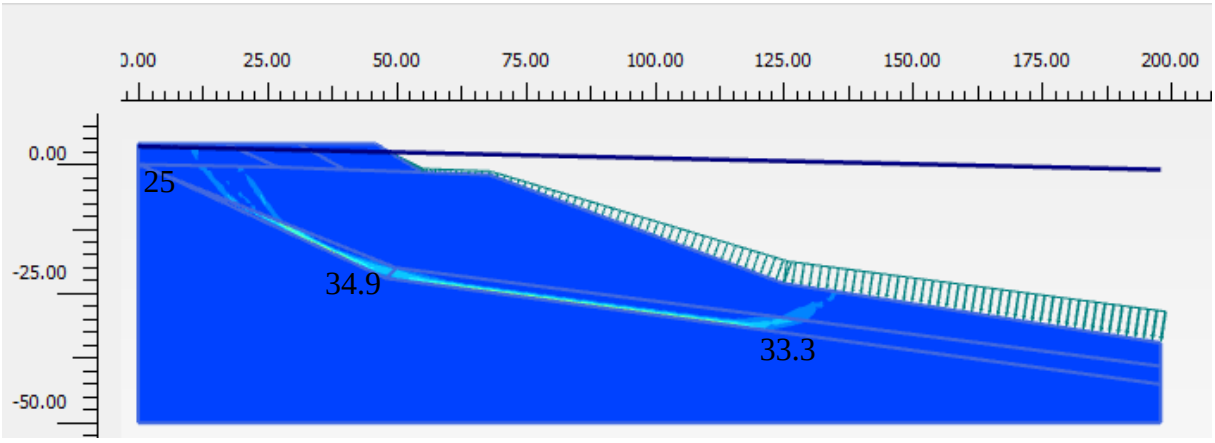

Figure 41: Failure mechanism for varying su in both clay layers. The undrained shear strength values are presented on the failure surface (unit kpa).

The failure mechanism in the case of undrained shear strength varying only in the lower layer is the one responding less with the failure in figure 38. The incremental strains are smaller than in the other cases and the shape of the failure mechanism is different. The failure surface is appearing under the fill, while in all the other cases it is beginning from inside the fill.

The failure mechanism in the case of undrained shear strength varying in both layers has the better correspondence with figure 38. This is normal because this is the scenario closest to the real slope properties.

6.3 Conclusions and further work

The main cause of the landslide in Sørkjosen was the filling in the sea at the pier. The filling, which was completed in November 2014, led to such a low level of stability that the area could not withstand the extra load it was exposed to due to heavy rainfall and heavy snowmelt on 10 May 2015.

Calculation were made in profile 31 in the pier and showed that the stability was critically low after the completion of the fill 6 months before the landslide with a computational safety factor close to 1.00.

The finite element method program Plaxis 2D was used, by simulating the filling works at the pier since 1994. Simulations for various undrained shear strength situations were generated, to determine the conditions that provide the most real- life failure mechanism. Chapters 6.1 and 6.2 describes the results of the simulations.

Undrained shear strength varying with depth for both clay layers is the scenario closest to reality (suA= 25 at the top of the higher layer and increasing with depth). In this case an important observation is the utilization of a negative su increment for the lower clay. This is normal because the overburden of the lower clay is smaller than the highest's one so the value of the undrained shear strength in the bottom of this layer should be lower than in the top.

Also, Mohr -Coulomb model seems to underestimate the strains in the failure mechanism (more plastic deformation) in comparison with the NGI-ADP model. The reason is explained in chapter 6.1.

The present study is not covering all aspects of the project. There are more tasks to be done in order to have a complete and scientific overview of the stability in the whole area in Sørkjosen. The proposed parameters should be used for back-calculations of other profiles near the area Jubelen. These calculations from other profiles could give combination of parameters, which should be compared with the proposed from the present study and differences should be discussed as well.

Also, it is recommended to model the landslide in Plaxis 3D for more complete analysis.

Finally, to avoid dangerous situations in the future it is critical that the shoreline areas along the coast of Norway, are mapped, especially the ones with clay presence. Individuals and

companies that wish to build in the beach zone should take lessons from previous landslides and take all precautions, with increased focus on investigation and mapping ahead.

Bibliography

Andersen, A. a. (1967). *Slides in subaqueous slopes in loose sand and silt.* . Norwegian Geotechnical Institute Publication 81.

Augarde C. E., L. A. (2003). . *Stability of an undrained plane strain heading revisited.*

Austefjord, S. (2016). *Skred i strandzonen:Studie av skredet i Indre Sokkelvik.* Trondheim.

BJORDAL, H. H.-O. (2011). *Skred og flom på veg : statistiske betraktninger.* Olso: Vegdirektoratet.

Bobrowsky, P. a. (2013). *The landslide Handbook-Guide to Understanding Landslides: Global risk Preparedness.* Springer.

Brænd, T. (1961). *Landslide catastrophe at Sokkelvik, Nord Reisa May 7th 1959.* TRONDHEIM: NGI.

Brinkgreve R.B.J., S. W. (2010). *PLAXIS 2D 2010 - General Information.* . Delft.

CLAGUE, J. J. (2013). *Encyclopedia of Natural Hazards.* Springer Netherlands.

COLLEUILLE, H. B. (2017). *Jordskredvarslingen: nasjonal varslingstjeneste for jord-, sørpe- og flomskredfare.* Oslo: NVE.

EILERTSEN, R. S.-S. (2012). *Submarine mass wasting and deposition in selected Norwegian fjord deltas* . Landslides and Engineered slopes, 1 .

Emdal A., S. N. (2015). *Geotechnics field and lab investigation methods.* Trondheim,Norway: NTNU.

Fauskerud, O. A. (2012). *Bruk av anisotropiforhold i stabilitetsberegninger i sprobruddmaterialer* . Oslo.

Feloni E. and Nastos, P. (2015). *Morphological analysis of the Aheloos river delta.* Athens.

Grimstad, G. A. (2012). *NGI-ADP : Anisotropic shear strength model for clay.*

H., D. E. (1968). *Theory of Plasticity and Failure of Soil Masses.*

HAMPTON, M. A. (1996). Submarine landslides. *Review of Geophysics* , 35-59.

HANSEN, L. L. (2011). *Turbiditic, clay-rich event beds in fjordmarine deposits caused by landslides in emerging clay deposits–palaeoenvironmentalinterpretation and role for submarine mass-wasting.*

HOVELSRUD, G. K. (2007). *Utviklingen av naturulykker som følge av klimaendringer : utredning på oppdrag fra Statens Landbruksforvaltning.* Olso; CICERO .

HUNGR, O. L. (2014). The Varnes classification of landslide types, an update. *Journal of the Internation Consortium on Landslides,11*, 167-194.

J.Locat, S. L. (2013). *Weak Layers: Their Definition and Classification from a Geotechnical Perspective.*

KVALSTAD, T. J. (2005). The Storegga slide: evaluation of triggering sources and slide mechanics. *Marine and Petroleum Geology. ,* 245-256.

L'Heureux J.S., N. S. (n.d.). *Revisiting the 1959 quick clay landslide at Sokkelvik, Norway.*

L'HEUREUX, J. S. (2012b). *Identification of weak layers and their role for the stability of slopes at Finneidfjord, Northern Norway.*

L'HEUREUX, J.-S. &.-N. (2009). *A multidisciplinary study of shoreline landslides : from geological development to geohazard assessment in the bay of Trondheim.* Norwegian University of Science and Technology, Department of Civil and Transport Engineering, Faculty of Engineering Science and Technology.

L'Heureux, J.-S. e. (2011). Landslides along Norwegian fjords, processes, cause and hazard assessement. *Proceedings of the 2nd world landslide forum.* Rome Google Scolar .

LONGVA, O. J. (2003). *The 1996 Finneidfjord slide; seafloor failure and slide dynamics.* Springer.

MASSON, D. W. (2010). *Large landslides on passive continental margins:processes, hypotheses and outstanding questions.* Springer.

Nesje, A. a. (1994). Erosion of Sognefjord, Norway.

Nordal S., L. J. (2016). *Final report of the investigation group after the slide in Sorkjosen 10th May 2015.* SINTEF report SBF20160043.

Nordal, S. (2018). *Geotechnical Enginnering Advanced course.* Trondheim: Norwegian University of Science and Technology.

Nordal, S. J.-S. (2016). *Lessons learned from the 2015 Soerkjosen shoreline landslide in Norway.*

Sandven, R. e. (2017). *Geotechnics Field and Laboratory Investigations.* Trondheim: NTNU.

SHRODER, J. F. (1971). *Landslides of Utah.* Utah Geological and Mineralogical Survey.

TALLING, P. C. (2014). *Large Submarine Landslides on Continental Slopes: Geohazards, Methane Release, and Climate change.*

Terzaghi, K. (1943). *Theoretical Soil Mechanics.* New York: Wiley.

Thakur, V. K. (2014). *En omforent anbefaling for bruk av anisotropifaktorer i prosjektering i norske leirer.*

Thakur, V. K. (2016). *A procedure for the assessment of the undrained shear strength profile of soft clays.* Proceedings of the 17th Nordic Geotechnical Meeting.

Thakur, V. L. (2014). *Landslide in sensitive clays* . Springer.

Theoretical Soil Mechanics . (2016). Norwegian University of Science and Technology.

VARNES, D. J. (1978). *Slope movement types and processes.* Special report, 176, 11-33.

APPENDIX A

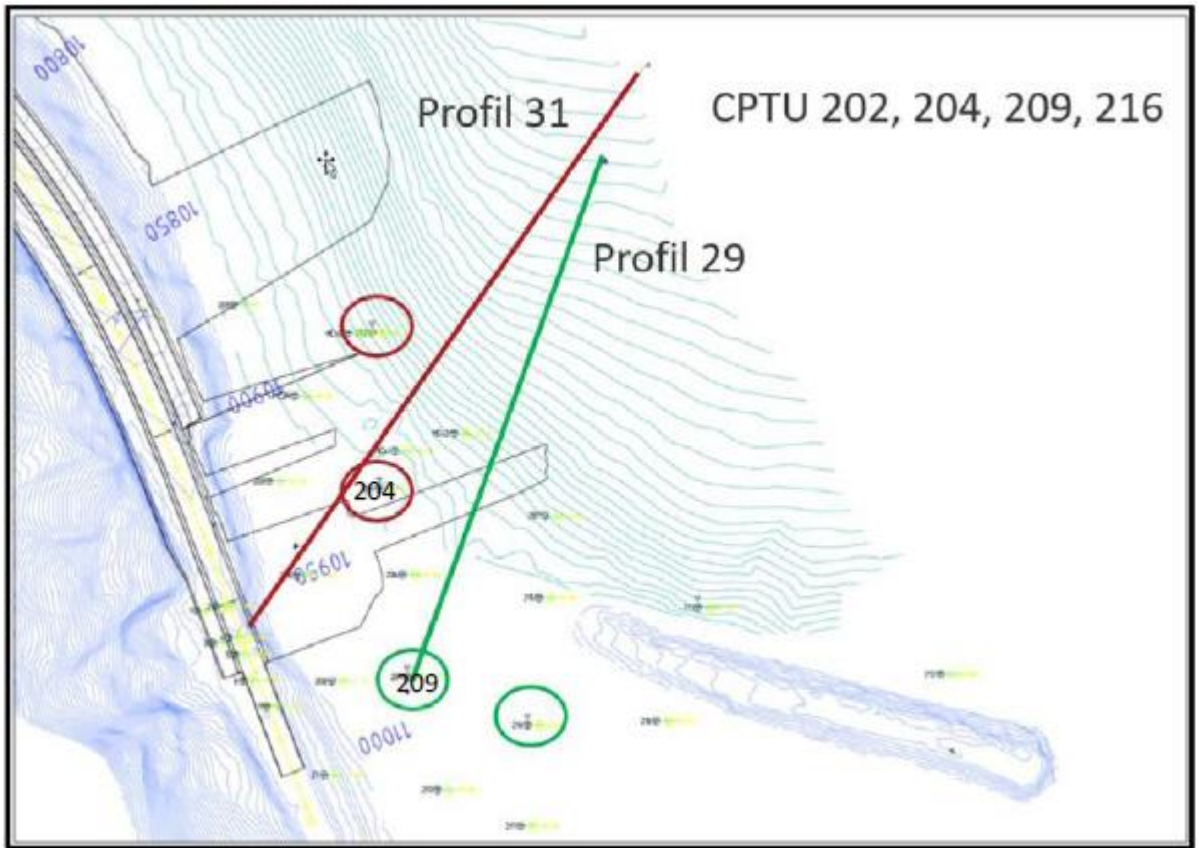

Profile 31 for stability calculations near the pier. (Nordal.S, L'Heureux.J, Skotheim. A, 2016)

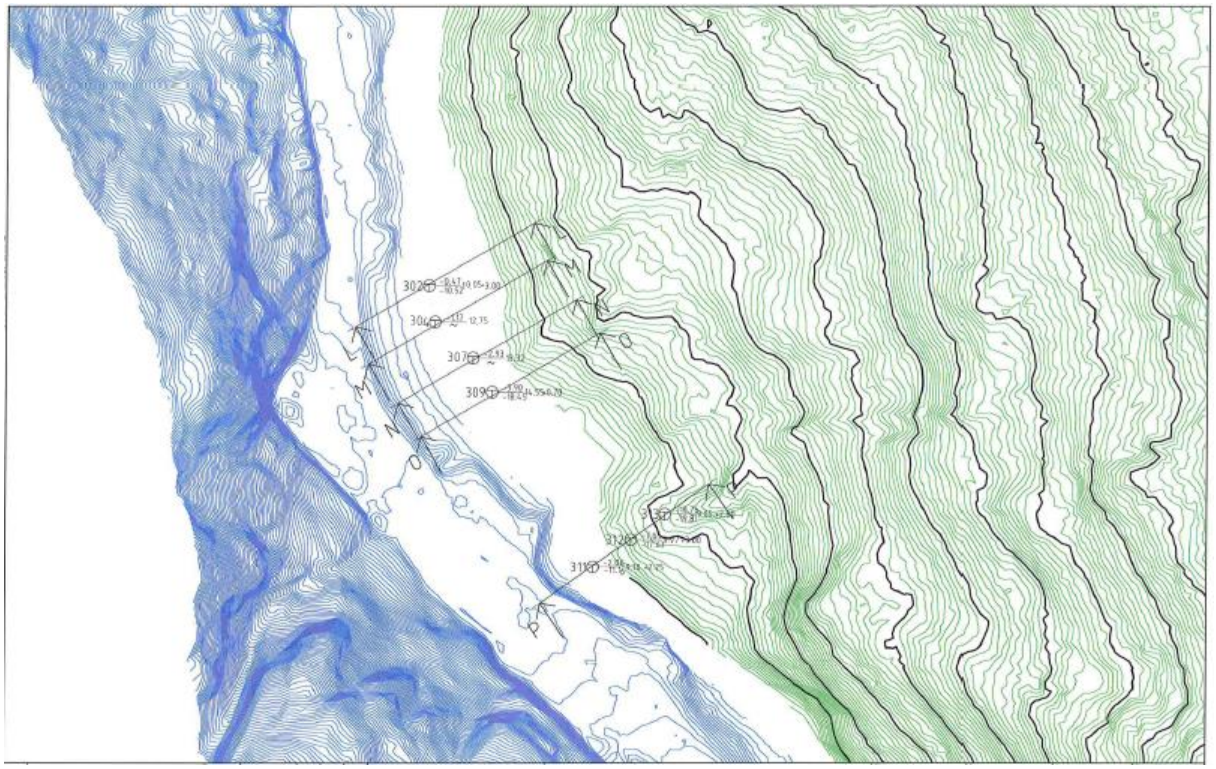

Drilling plans. (Nordal.S, L'Heureux.J, Skotheim. A, 2016)

APPENDIX B

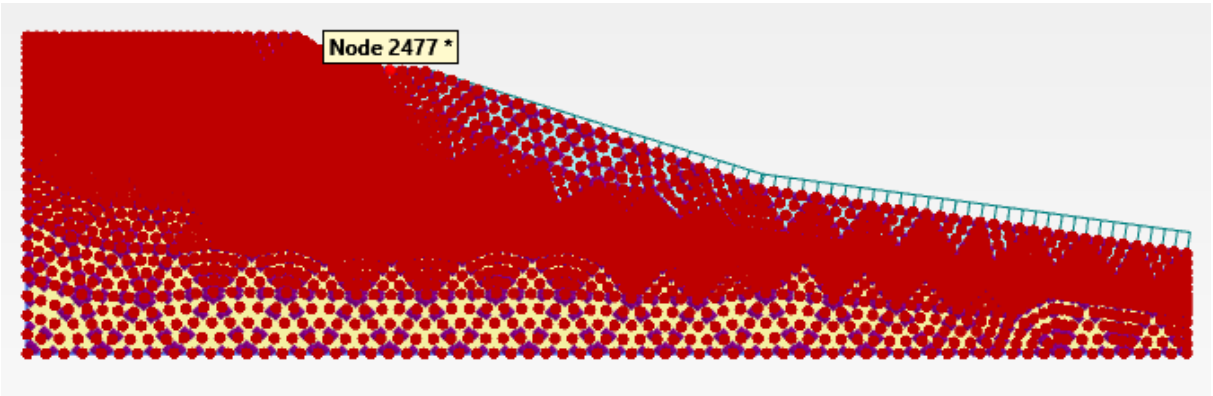

Node used for stability calculations.